CARBON-RICH CARBORANES AND THEIR METAL DERIVATIVES

RUSSELL N. GRIMES

Department of Chemistry, University of Virginia, Charlottesville, Virginia

I. Introduction

Interplay between experiment and theory is a basic feature of science, and the field of boron cluster chemistry since the 1960s provides a

ISBN 0-12-023626-5

fascinating illustration of this process (*17, 21, 22, 24, 45, 66*). The boron hydrides, with their peculiar, unconventional cage-like structures, have intrigued theorists for years, even as the degree of interest exhibited in them by industry and government has waxed and waned (and recently waxed again). Because boron has four valence orbitals but only three electrons, its binary hydrides have fewer than one electron pair per bonding interaction, yet they hold together very nicely by the trick of electron delocalization; that is, some of the electrons are not constrained to ordinary Lewis-type bonds between pairs of atoms (so-called two-center bonds), but can extend over three atoms (three-center B—B—B and B—H—B bonds). In fact, in some types of boranes electrons are effectively delocalized over the entire cage framework, as in the icosahedral $B_{12}H_{12}^{2-}$ system and its analogous carborane $C_2B_{10}H_{12}$ (*45*).

In order to facilitate this electron delocalization, borane molecules adopt cluster shapes that permit high connectivities between boron atoms and thus make the most efficient use of the available electrons. Hydrocarbons, in contrast, have exactly the right numbers of electrons for *localized* two-center bond networks of carbon and hydrogen atoms. Here, there is no need for clustering; indeed, the most favorable arrangements are chains and rings, which allow each carbon atom to use its four valence orbitals and to acquire a full octet of valence electrons.

Boranes and hydrocarbons thus represent two extremes in network bonding systems. But what happens when carbon is incorporated into a polyhedral borane framework? The answer to this question has been emerging since the early 1960s, during which time vast new areas of synthetic and structural chemistry have been opened for exploration and numerous types of molecular geometry that were not even conceived previously have been shown to have stable existence. An oversimplified summary is as follows. When boron is the dominant structural element and the number of available bonding electrons is not sufficient for a classical hydrocarbon-like chain or ring structure (a so-called electron-deficient condition), the cluster motif is followed; this is the case in the polyhedral carboranes of the $C_2B_{n-2}H_n$ class (known for $5 \leq n \leq 12$) and their $B_nH_n^{2-}$ counterparts ($6 \leq n \leq 12$). In many carboranes, such as the extremely stable icosahedral $C_2B_{10}H_{12}$ isomers, carbon often adopts a role quite out of character from the viewpoint of organic chemists, by assuming a coordination number of five or six. On the other hand, cage systems containing mostly carbon with an occasional boron atom or two naturally tend to adopt hydrocarbon-like geometries; examples are boradamantane and borabenzene, which

have the classical (Lewis) structures of their organic namesakes and are properly described as organic heterocycles (*67*).

Is there an intermediate region of composition and structure in which one encounters stable "hybrid" geometries that exhibit both borane-like and hydrocarbon-like features within the same molecular framework? There is, and it is to this class of compounds that the present chapter is directed. In these "carbon-rich" carboranes, most of which have four skeletal carbon atoms in a borane matrix, some truly novel patterns of structure and reactivity have been observed (*18, 19*). This chemistry grew primarily out of a discovery in 1974 in the author's laboratory, by two former postdoctoral associates, Vernon Miller and William Maxwell (*53*), and was subsequently developed by a series of other able postdoctoral and graduate students. This work is far from complete—indeed, it must be regarded as still in an exploratory phase—but it has progressed to a point where a summary appears warranted. The current body of structural and spectroscopic data on four-carbon carboranes and metal complexes, which includes some two dozen X-ray crystal structures, provides a reasonable basis for discerning patterns in bonding and geometry; moreover, the stereochemistry involved is sufficiently different from that in "ordinary" carborane systems as to justify separate treatment.

Before we turn to the subject at hand, some perspective may be helpful. Hundreds of carboranes and metallacarboranes are now known, the vast majority of which (at least 95%) contain two skeletal carbon atoms. The dominance of the dicarbon species reflects primarily the fact that most carboranes are prepared via incorporation of alkynes into borane skeletons; however, a few one-carbon species have also been characterized. In the main, the structures of these one- and two-carbon polyhedral carboranes are reasonably well accounted for by the skeletal electron-count theory (see Section II), which was developed in the 1970s. In nearly all cases the observed cage structures are either closo polyhedra (all faces triangular) or fragments thereof, in accordance with theory. But what would be the structural consequences if, starting with a carborane such as icosahedral $C_2B_{10}H_{12}$, one were successively to replace boron atoms with carbon atoms, forming species such as $C_3B_9H_{12}$, $C_4B_8H_{12}$, $C_5B_7H_{12}$, and so on? According to the general rules of electron counting in clusters, the cage structure would be expected to become progressively more open as the carbon content, and hence the skeletal electron population, increased; however, one could not have said with confidence just what form this cage opening might take. Actually, there is no known way to perform such step-by-step

carbon substitutions, but, in the 1974 work already mentioned, we unexpectedly found a way to make *C*-alkyl derivatives of $C_4B_8H_{12}$ in high yield. Subsequently, Freyberg *et al.*, in our laboratory, determined the structure of $(CH_3)_4C_4B_8H_8$ by X-ray diffraction and found a distorted icosahedral geometry with two open faces (*16*)—a type of cage structure not previously known and certainly not predicted by anyone. Even more unexpectedly, we found that when $(CH_3)_4C_4B_8H_8$ is dissolved in common polar or nonpolar solvents, it partially and reversibly rearranges to a different isomer, as shown in NMR spectra; when the solvent is evaporated, the solid compound reverts to its original structure (*52*).

These discoveries led to numerous others that were scarcely less surprising, many of which have involved metal insertion into tetracarbon carborane polyhedra. In the early part of this work we were confronted with a growing collection of odd structures in which it was difficult to see an underlying pattern, but now, with a considerable body of chemical and spectroscopic data in hand, the dust is gradually clearing. The key point, on which we shall elaborate, is that *local carbon–carbon and carbon–metal interactions within the skeletal framework* profoundly influence cage geometry in these carbon-rich systems. In the dicarbon carboranes, such local effects are much less evident as a rule. For example, isomers of a given dicarbon cage system, such as $(\eta^5\text{-}C_5H_5)CoC_2B_9H_{11}$, normally have the same polyhedral shape and differ only in the location of heteroatoms (in this case, cobalt and carbon) on the cage surface; in contrast, isomers of tetracarbon species often exhibit very dissimilar gross geometries.

The different character of the carbon-rich carboranes, relative to the well-developed dicarbon carborane field, is not restricted to structure alone but is also reflected in some unique chemistry that will be described below. Section II deals with the theory of structure in boron clusters as it applies to the subject of interest here.

II. Structural Patterns in Carboranes: General Considerations

Bonding and molecular structure in borane frameworks have been treated by numerous authors from many different viewpoints, and no attempt will be made here to deal with this subject in detail. Rather, our purpose will be to provide sufficient background to allow rational discussion of the chemistry and geometry of carbon-rich carboranes to be described later.

A. Valence-Bond Descriptions

It will be assumed that readers of this chapter have some familiarity with the localized-bond description of the boron hydrides developed by Lipscomb and co-workers [and which led ultimately to a Nobel award to Lipscomb in 1976; (*45*)]. In this approach, a borane framework is viewed as a collection of BH units bound together by some combination of two-center B—B and three-center B—B—B bonds; the number of each type depends on the number of available valence electrons in the molecule. "Extra" hydrogen atoms are attached either to B—B edges (forming B—H—B three-center bridge bonds), or to individual BH groups, converting them to BH_2 units. Because each boron atom has four valence orbitals and each hydrogen one, the number of allowed bonding descriptions for a given borane is obviously limited, in some cases to a single structure. Further constraints are given by considerations of valence bond angles. These ideas have been formulated quantitatively in the famous *equations of balance* (*45*), which are now found even in some undergraduate inorganic texts.

Figure 1 depicts the localized-bond description of hexaborane(10), B_6H_{10}, together with its actual molecular structure. Note that in drawing the molecular geometry (Fig. 1b) we represent all the bonded connections by single lines, irrespective of the actual electron distribution; this is standard practice and is followed throughout this chapter (except when, as in Fig. 1a, we wish to present explicitly a localized-bond arrangement). In comparing Figures 1a and 1b it will be seen that, although the apex boron atom is six-coordinate, it is only tetravalent, that is, it is involved in only four electron-pair bonds, as indeed it must be because boron, like carbon, has only four valence orbitals.

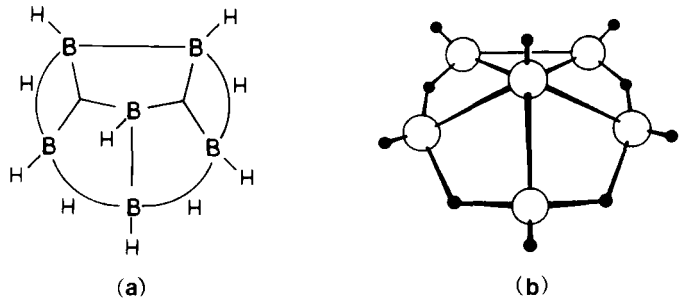

FIG. 1. (a) Localized bonds in B_6H_{10}. (b) Molecular structure of B_6H_{10} (*45*).

It will be noted that the B_6H_{10} structure in Fig. 1a has four B—H—B three-center bonds, two B—B two-center bonds, two B—B—B three-center bonds, and no BH_2 groups; in shorthand form this is referred to as a 4220 structure (*45*). The eight bonds require a total of 16 electrons, which is exactly the number available: of the total of 28 valence electrons in the molecule, 12 are required for the six localized B—H bonds, leaving the remaining 16 to bind the six BH units and the four extra hydrogens together. Other possible bonding schemes could be written, for example, 3311 and 2402 (note that in each instance the total of the digits must equal the number of bonds, in the present case, eight). However, these latter possibilities are eliminated by the known molecular structure (Fig. 1b), which contains four bridging hydrogens and no BH_2 groups; hence the 4220 arrangement (Fig. 1a) is correct.

In many cases, particularly in large or highly symmetric molecules, resonance descriptions involving several different arrangements may be required. Also, in recent years detailed theoretical studies have provided support for the concept of "fractional" three-center bonds (see later discussion), wherein particular groups of atoms may be linked by only part of an electron pair (*8*); such concepts have increased the utility of the localized-bond theory, for example, in calculating charge distributions. However, for present purposes we shall not require these more sophisticated refinements of the theory.

If one replaces a boron atom with carbon in the cage framework, at the same time removing a hydrogen atom to maintain the number of electrons constant, the same type of localized-bond description can in principle be employed. This is illustrated in Fig. 2 for the carborane 2,3-$C_2B_4H_8$, which is an analog of B_6H_{10}. The molecular structure of 2,3-$C_2B_4H_8$ (the prefix numbers of which designate the carbon locations) is shown in Fig. 2a, and it resembles that of B_6H_{10} (Fig. 1b), except that there are only two B—H—B bridges rather than four. This, of course, requires a different localized-bond description from that in

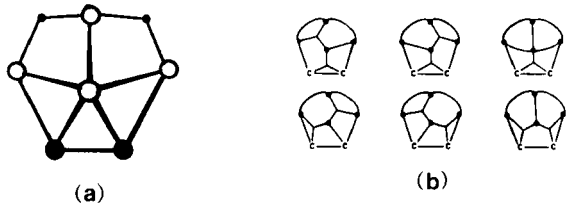

FIG. 2. (a) Molecular structure of 2,3-$C_2B_4H_8$. ○, BH; ●, CH; •, H. (b) Some localized valence structures for 2,3-$C_2B_4H_8$ (*49*). Reprinted from *J. Am. Chem. Soc.* **94**, 8699. Copyright 1972 American Chemical Society.

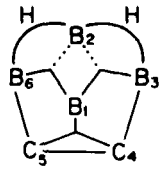

FIG. 3. Fractional three-center bond description of $2,3\text{-}C_2B_4H_8$ (*49*). Reprinted from *J. Am. Chem. Soc.* **94**, 8699. Copyright 1972 American Chemical Society.

Fig. 1a, and several possible structures (*49*) are shown in Fig. 2b. Alternatively, a fractional three-center bond description (*49*), given in Fig. 3, is in reasonable accord with quantitative molecular orbital treatments.

The molecule $2,3\text{-}C_2B_4H_8$ is but one member of a series of isoelectronic molecules analogous to B_6H_{10} (Fig. 4). All of these are known either as parent species or alkyl derivatives, and all can be described in terms of localized bonds, if desired. This group of molecules rather dramatically illustrates the importance of fundamental principles of bonding and structure that provide a common thread linking such apparently unrelated species as B_6H_{10} and $C_6(CH_3)_6^{2+}$.

The placement of carbon atoms in the structures in Fig. 4 is highly significant, as it demonstrates several trends that are well established in carborane structural chemistry. The two most important observations are that *carbon tends to occupy low-coordinate vertices when possible* and that *bridging hydrogen atoms are located between boron atoms only;* no clear examples of discrete B—H—C or C—H—C bridges

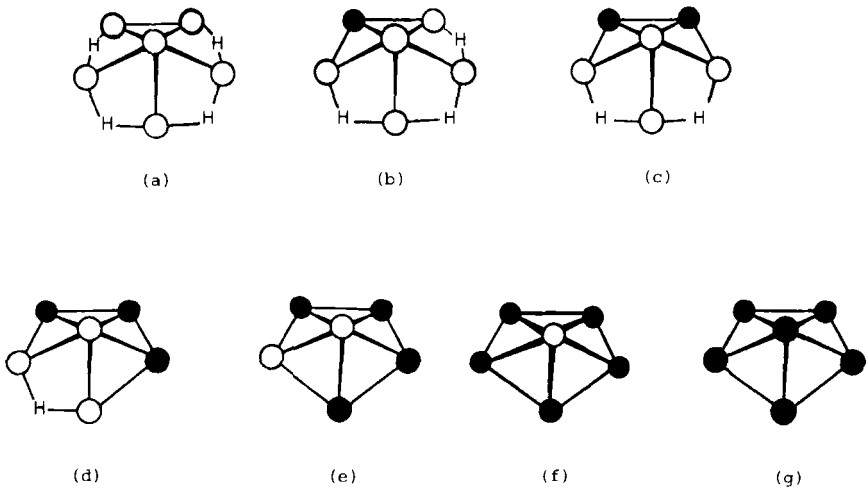

FIG. 4. Isoelectronic series of 6-vertex nido species. (a) B_6H_{10}, (b) CB_5H_9, (c) $C_2B_4H_8$, (d) $C_3B_3H_7$, (e) $C_4B_2H_6$, (f) $C_5BH_6^+$, (g) $(CH_3)_6C_6^{2+}$. ○, BH; ●, CH or CCH_3.

have been found. Other generalizations regarding the structural role of carbon will be presented later.

B. Molecular Orbital Descriptions and Electron-Counting Rules

Localized-bond treatments of the sort illustrated in Section I,A work well for open-cage molecules, particularly small ones where the number of allowed structures is limited. For closo (completely triangulated) cages, however, localized descriptions tend to become cumbersome and make it difficult to gain qualitative insight into the bonding, to rationalize structures, and to see relationships among different molecular species. Consequently, the closo systems, which are regarded in general as highly electron-delocalized, are commonly treated in molecular orbital (MO) terms. Quantitative MO studies have for the most part been centered on the binary borane clusters such as the polyhedral $B_nH_n^{2-}$ ions, but conclusions reached for these systems can usefully be transferred to their carborane (and other heteroborane) counterparts; thus both icosahedral $B_{12}H_{12}^{2-}$ and its analog, $C_2B_{10}H_{12}$, have 13 bonding skeletal molecular orbitals which precisely accommodate the 26 electrons available for cage bonding.

These studies of the $B_nH_n^{2-}$ series and related clusters have established a very important rule: closo n-vertex polyhedra composed of units such as BH and CH, which supply three valence orbitals for framework bonding (the fourth orbital being utilized for linkage to hydrogen) have $n + 1$ skeletal bonding MOs (*46, 65, 79, 88*). If $n + 1$ electron pairs are available to fill these orbitals, a stable closed-shell system should result. Hence, *n-vertex clusters having 2n + 2 electrons for cage bonding are predicted to have closo geometry*. Additional electrons beyond the quota of $2n + 2$ must occupy antibonding orbitals, leading to distortion; normally, this distortion takes the form of cage opening to produce a cluster with one or more open (i.e., nontriangular) faces. An equivalent way of describing this is to observe that, if one removes a vertex from an n-vertex closo system, the *absolute* number of bonding MOs is unchanged, but because the value of n has been reduced, the number of bonding MOs must be given as $n + 2$. Thus both octahedral $C_2B_4H_6$ ($n = 6$) and square-pyramidal $C_2B_3H_7$ ($n = 5$) have 7 skeletal bonding MOs, represented as $n + 1$ in the former case and $n + 2$ in the latter.

Clusters that correspond to closo polyhedra minus one vertex are labeled *nido* (Greek for *nest*); examples are the square pyramid and the pentagonal pyramid. Clusters representing closo polyhedra minus *two*

vertices are classified *arachno* (*web*), and for three missing vertices the term is *hypho* (*net*). Hence the skeletal electron requirements for closo, nido, arachno, and hypho species are $(2n + 2)$, $(2n + 4)$, $(2n + 6)$, and $(2n + 8)$, respectively.

The number of skeletal electrons in the cage is the sum of contributions from all the units, assuming that bonds external to the polyhedron are not involved; thus, BH, CH, and NH groups contribute 2, 3, and 4 electrons, respectively; a "bare" nitrogen atom is a 3-electron donor if the presence of an exopolyhedral lone pair is assumed. Transition metal–ligand units such as $Co(\eta^5\text{-}C_5H_5)$, $Fe(CO)_3$, and $Ni(\eta^5\text{-}C_5H_5)$ contribute, respectively, 2, 2, and 3 electrons; here several things are taken for granted: (1) the metal, like B or C, utilizes three orbitals for bonding to the cage skeleton; (2) the metal acquires an 18-electron configuration; and (3) metal orbitals that are not used for bonding to the cage or to external ligands are nonbonding and are filled with electrons. Because $Co(\eta^5\text{-}C_5H_5)$ and $Fe(CO)_3$ are both 2-electron donors, one expects that they could replace BH in borane frameworks, and indeed this is a very common occurrence; B_5H_9 analogs such as 1- and 2-$(\eta^5\text{-}C_5H_5)CoB_4H_8$ and 1-$(CO)_3FeB_4H_8$, B_6H_{10} analogs such as 1- and 2-$(CO)_3FeB_5H_{10}$ and 1-$(\eta^5\text{-}C_5H_5)CoB_5H_9$, $C_2B_{10}H_{12}$ analogs such as $(\eta^5\text{-}C_5H_5)_2Co_2C_2B_8H_{10}$ and $(\eta^5\text{-}C_5H_5)_2Ni_2B_{10}H_{10}$, and hundreds of other examples have been thoroughly characterized (*17, 22, 66*). These ideas have received considerable support from detailed MO studies and, most importantly, from a large body of experimental evidence.

The skeletal electron-count theory was originated by Wade (*88*) and is based on concepts inherent in the Lipscomb valence-bond treatment of boranes and carboranes (*45, 46*), and it received important contributions from Mingos (*65*) and Rudolph (*79*); in addition, a number of other authors have elaborated on various aspects of cluster bonding (*20, 44, 71, 90*). In recent years it has become clear that the theory is broad in scope and can usefully be applied to metal clusters and other nonboron systems, with some modifications. Nevertheless, major limitations of this approach have become apparent in certain types of boron clusters, including the tetracarbon carboranes. We turn now to a consideration of this problem.

C. Structure and Bonding in Carbon-Rich Cage Systems

The simple closo–nido–arachno classification of clusters, described in Section II,B, works well for boranes, dicarbon carboranes, and their metal derivatives. Most such clusters are readily identifiable as stand-

ard closo polyhedra or polyhedral fragments, and there is a clear correlation between the cage geometry and the skeletal electron population, as was outlined previously. Where "violations" of the electron-counting rules occur, these usually involve heavy metals such as platinum, species of high metal content in which local metal–metal interactions are important [e.g., $(\eta^5\text{-}C_5H_5)_4M_4B_4H_4$ (M = Co, Ni)] or halogenated clusters (halogen substituents tend to donate electron density into the cage and thus alter the skeletal electron population).

The carbon-rich carboranes present an altogether different situation and illustrate three major limitations of the skeletal electron-counting theory as presented: (1) it predicts only thermodynamically favored structures and cannot anticipate kinetically stabilized cage geometries; (2) even when the structural class (e.g., nido) is correctly assigned, the theory may not be able to specify which particular geometry is to be expected; and (3) because the theory assumes electron delocalization over the entire cluster, it cannot easily handle situations involving local bonding interactions in portions of the cluster framework. The extent of this problem varies considerably with cluster size and number of valence electrons. For example, all known 12-vertex, 26-electron clusters are icosahedral (closo), and all 11-vertex, 26-electron clusters have a nido geometry, corresponding to an icosahedron minus one vertex (Fig. 5). These structures are exactly in accord with the presence of $2n + 2$ and $2n + 4$ electrons, respectively, and illustrate the fact that the icosahedron is the overwhelmingly preferred arrangement for 26-electron systems.

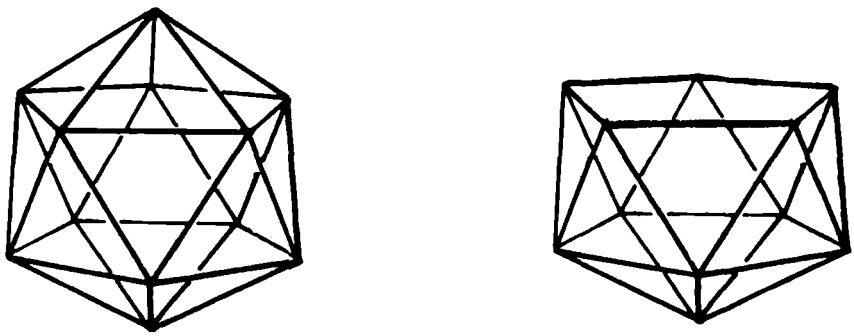

FIG. 5. (a) Icosahedron. (b) Nido icosahedral fragment.

In dramatic contrast, consider the 28-electron, 12-vertex clusters. According to theory, these are $(2n + 4)$-electron systems and formally belong to the nido classification; thus we would expect them to adopt an open-cage geometry derived from a 13-vertex closo polyhedron by removal of one vertex (Fig. 6). What we find, actually, is that the known 12-vertex, 28-electron systems adopt a wide variety of different shapes, comprising at least seven different structural types [Fig. 7; (*59*)]. Of these, all except types 1 and 7 involve four-carbon carboranes or metallacarboranes. The three compounds of type 5 have the "expected" nido geometry, corresponding to Fig. 6b; the others are widely divergent and can be described as distorted icosahedra. Particularly noteworthy is the fact that the three isomers of $(\eta^5\text{-}C_5H_5)Co(CH_3)_4C_4B_7H_7$ fall into three different structural classes (types 4–6). It should be stressed that the classification of structural types in Fig. 7 is based on *distinct differences in connectivity;* formal conversion of any of these geometries to any other requires bond breakage and bond formation, as opposed to mere "distortion."

The species illustrated in Fig. 7 are a somewhat motley collection with diverse origins; some clearly do not represent thermodynamically favored structures, but all are reasonably heat- and air-stable (the two isomers of $R_4C_4B_8H_8$, types 2 and 3, are in equilibrium in solution at room temperature).

We shall defer detailed discussion of the individual structures to a

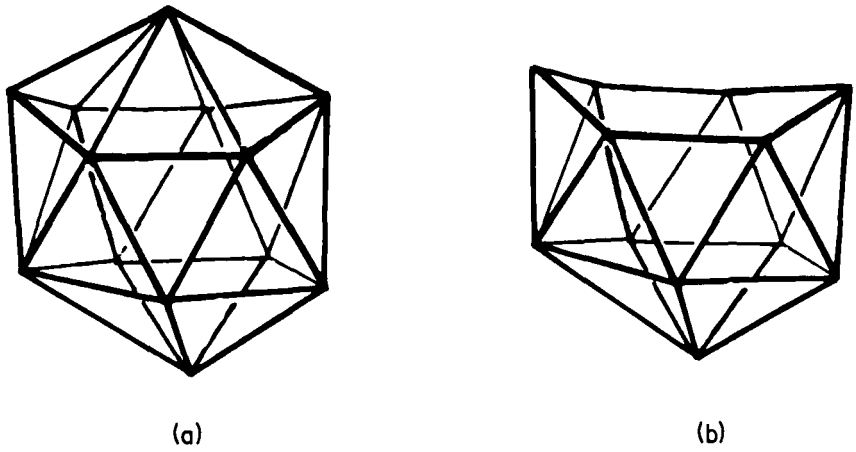

FIG. 6. (a) 13-Vertex closo polyhedron (docosahedron). (b) Nido 12-vertex cage formed by removal of a six-coordinate vertex from a closo 13-vertex polyhedron.

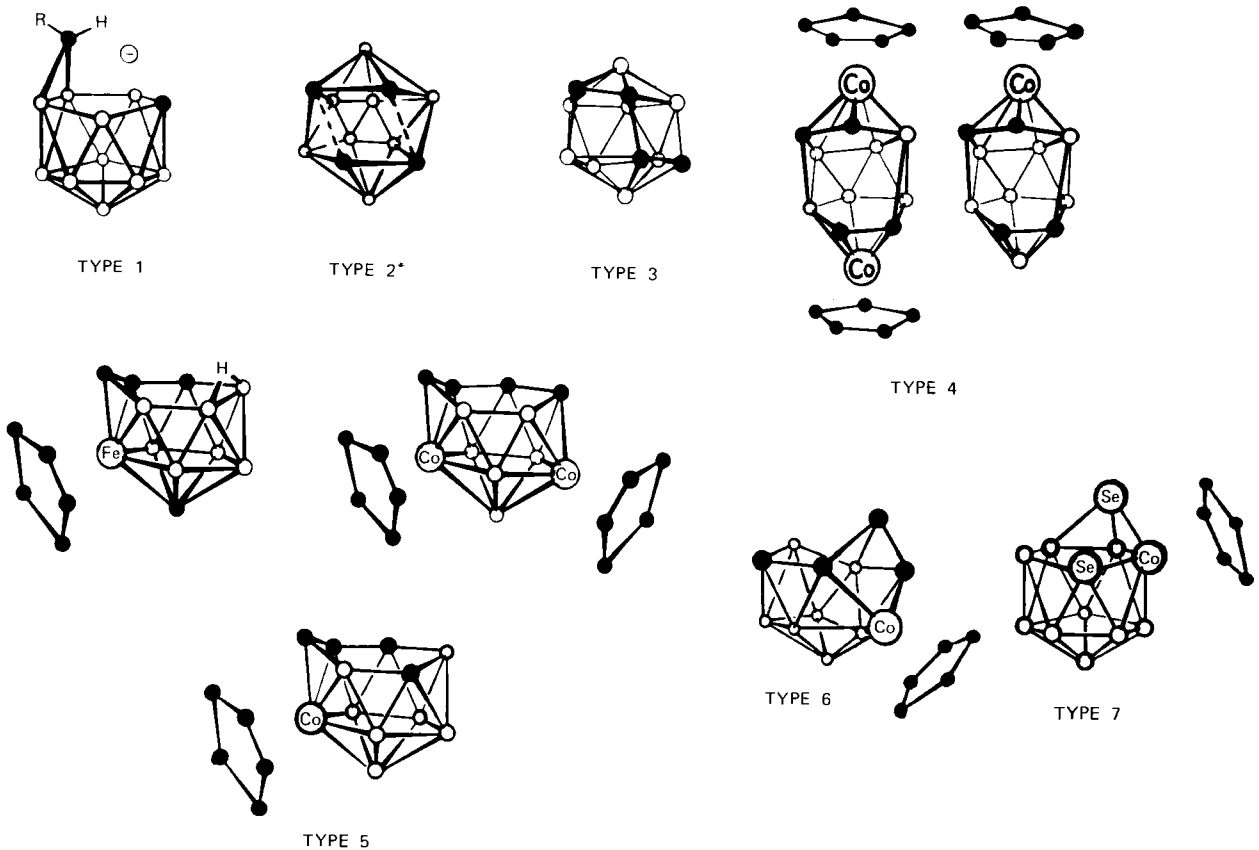

FIG. 7. Structural types of 12-vertex 28-electron cages (*59*). *, NMR only; ○, BH; ●, CH or CCH_3. Reprinted from *Inorg. Chem.* **20,** 1201. Copyright 1981 American Chemical Society.

later point, but several general observations can be made here. First, the observed differences in cage geometry cannot be ascribed solely, or even mainly, to differences in elemental composition; this is shown by the existence of three different structural isomers of $(\eta^5\text{-}C_5H_5)Co(CH_3)_4C_4B_7H_7$, as mentioned previously. Moreover, in the 26-electron, 12-vertex family there is only one observed geometry—icosahedral—despite wide variation in elemental composition. Second, it is clear that a major factor determining structure in these systems (particularly the metal-containing ones) is the *synthetic origin;* we shall have more to say on this. Third, the apparent thermodynamically favored geometry for 12-vertex, 28-electron *metallacarboranes* (but not carboranes) is that shown as type 5 (Fig. 7), which is the nido geometry that would have been expected from electron-counting arguments in the first place. Hence, to this limited degree the structural theory is in accord with observation for the 12-vertex nido case. Finally, an important point: these carbon-rich cage structures are clearly beyond the scope of quantitative MO calculations, and hence this is an area in which understanding can be gained only through a combination of experimental study and shrewd qualitative insight. In this field, the experimentalist unquestionably leads the way.

The 12-vertex, 28-electron systems in Fig. 7 represent only a portion of the four-carbon carborane and metallacarborane structures that have been established, albeit a major portion. With a single exception, $(\eta^5\text{-}C_5H_5)Co(C_6H_5)_4C_4B_3H_3$, an 8-vertex arachno species (see later discussion), all of the structural investigations in this area involve 26-, 28-, or 30-electron cages of 11–14 vertices. Table I classifies these compounds according to electron count and number of vertices and indicates, by code, the coordination numbers of metal and carbon atoms in each of the established structures. In all but a few instances the structures are known with certainty from X-ray diffraction studies; those characterized only by NMR data are enclosed in brackets.

All of the molecules in Table I contain four skeletal carbon atoms and were derived from $(CH_3)_4C_4B_8H_8$ or $(C_2H_5)_4C_4B_8H_8$ by synthetic routes outlined in the following discussion. No significance can be attached to the relative number of species in the various categories, but the table does indicate where the bulk of our structural information lies at the time of this writing. The available structural data reveal some significant patterns with respect to the stereochemistry of metal and carbon atoms in the cage framework, and we shall discuss these in the latter part of the chapter, following a description of synthetic routes and some chemistry of individual clusters.

TABLE I

STRUCTURALLY CHARACTERIZED 11- TO 14-VERTEX CARBON-RICH CARBORANES AND METALLACARBORANES[a,b]

Number of skeletal electrons	11-Vertex systems	12-Vertex systems	13-Vertex systems	14-Vertex systems
30	$2n$ + 8 electrons	$2n$ + 6 electrons $Me_4C_4B_8H_9^-$ 2444(4,6)[b] (cobaltocenium derivative)	$2n$ + 4 electrons $CpCrEt_4C_4B_8H_8$ 6-3445(5)[b] $(Ph_2PCH_2)_2NiMe_4C_4B_8H_8$ [Isomer **I:** 5-4445(5)] $[CpCoMe_4C_4B_8H_8]$ 5-4445(5) $[Me_2C_2B_4H_4]CoMe_4C_4B_8H_7 \cdot$ THF 6-4445(5)	$2n$ + 2 electrons $Cp_2Fe_2Me_4C_4B_8H_8$ Isomer **I:** 66-4445(5)[b] Isomer **II:** 66-4445(4) *Isomer **V:** 66-4455(5) *[Isomer **VII:** 66-5555(0)] **[Isomer **VIII:** 66-5555(0)] *Thermal rearrangement product **Final product of thermal rearrangement
28	$2n$ + 6 electrons $Me_4C_4B_7H_8Br$ 2444(5,5)	$2n$ + 4 electrons $CpCrEt_4C_4B_7H_7$ 6-3444(6) Type 2 (see Fig. 7) $Et_4C_4B_8H_8$ 3344(6) [$Cp_2Co_2C_4B_6H_{10}$, isomer **VI**] 55-4444(4)? Type 3 $Me_4C_4B_8H_8$ 4444(4,4) $Me_4C_4B_8H_7$-C_5H_4FeCp 4444(4,4)	$2n$ + 2 electrons	$2n$ electrons

		Type 4 $Cp_2Co_2Me_4C_4B_6H_6$, Isomer **V** 55-3344(6) $CpCoMe_4C_4B_7H_7$, Isomer **I** 5-3344(6) $CpCoMe_4C_4B_7H_6$-OEt, Isomer **I** 5-3344(6) Type 5 $CpFeMe_4C_4B_7H_8$ 6-3445(6) *$CpCoMe_4C_4B_7H_7$, Isomer **III** 6-3444(6) $Cp_2Co_2C_4B_6H_{10}$, Isomer **VII** 56-3444(6) Type 6 $CpCoMe_4C_4B_7H_7$, Isomer **II** 5-3444(4,5) *Thermal rearrangement product		
26	$2n$ + 4 electrons $CpCoMe_4C_4B_6H_6$ Isomer **I:** 5-4444(5) Isomer **II:** 4-4444(5)	$2n$ + 2 electrons	$2n$ electrons	$2n$ − 2 electrons

[a] All species have been characterized by X-ray diffraction, except those enclosed in brackets; structures of bracketed compounds are assigned from NMR evidence. Abbreviations: Cp, η^5-C_5H_5; Me, methyl; Et, ethyl; Ph, phenyl.

[b] Structure Code: Digits represent coordination numbers (with respect to the cage framework only) of nonboron atoms in the skeleton; those to left of hyphen are metals, those to right of hyphen are carbon. Underlined digits indicate location on an open face (double-underlined atoms are on two open faces). Digits in parentheses denote the number of atoms on the open face, or faces, in the cage. Example: for $Cp_2Fe_2Me_4C_4B_8H_8$, isomer **II** (Fig. 31b) 66-4445(4) signifies that the cage has two 6-coordinate metal atoms (one on an open face), three 4-coordinate carbons (two of them on open faces), and a 5-coordinate carbon; the molecule has a single 4-membered open face.

III. Small Three- and Four-Carbon Carborane Systems

As the foregoing discussion makes clear, this chapter is concerned primarily with the large C_4B_8 carboranes and their metallacarborane derivatives. The smaller C_3 and C_4 carboranes fall into a somewhat different category in terms of chemistry and geometry, and very few of them have been structurally characterized by diffraction methods. However, a brief outline of their syntheses is presented in this section.

A. Three-Carbon Carboranes

The reaction of tetraborane(10), B_4H_{10}, with acetylene in the vapor phase at 25–50°C produces small quantities of *C*-methyl and *C,C'*-dimethyl derivatives of 2,3,4-$C_3B_3H_7$, characterized from NMR spectra as a pentagonal pyramid with the three carbons in adjacent basal locations [Fig. 4(d)] (*26*). A kinetic study of this reaction (*15*) indicated that the initial step is formation of the unstable species B_4H_8, which adds four C_2H_2 units in stepwise fashion to form a solid polymer (the main product); side reactions, involving rearrangement of the $B_4H_8(C_2H_2)_x$ intermediates, evidently yield $C_3B_3H_7$ derivatives. The monomethyl compound, 2-$CH_3C_3B_3H_6$, on treatment with NaH loses its B—H—B bridging proton to form the $CH_3C_3B_3H_5^-$ anion, which in turn reacts with bromomanganese pentacarbonyl to form initially a red $(CO)_5Mn—(CH_3)C_3B_3H_5$ intermediate; at 100°C this complex loses CO to produce yellow *closo*-1,2,3,4-$(CO)_3Mn(CH_3)C_3B_3H_5$ (*40*). The same manganacarborane product can be prepared by reaction of neutral 2-$CH_3C_3B_3H_6$ with $Mn_2(CO)_{10}$ at elevated temperature (*40*).

The only other reported example of a three-carbon carborane is the strange species $C_3B_5H_7$, a colorless solid (mp 37°C) obtained in 15–20% yield by pyrolysis of the *nido*-carborane silyl derivatives μ- or 4-$SiH_3C_2B_4H_7$ (*84*). From spectroscopic evidence a fluxional closo cage structure has been proposed for $C_3B_5H_7$, with one of the framework carbon atoms lacking a hydrogen substituent. No further studies of this species have been reported.

Three-carbon metallacarboranes have also been prepared from alkyl derivatives of 1,3-diborolene, $C_3B_2H_6$, a five-membered ring system. Both nido 6-vertex monometallic complexes and closo 7-vertex dimetallic complexes (triple-decker sandwiches) have been characterized. Thus treatment of 1,3,4,5-tetraethyl-2-methyl-1,3-diborolene with nickelocene or $[(\eta^5\text{-}C_5H_5)Ni(CO)]_2$ gives orange-red $(\eta^5\text{-}C_5H_5)Ni(CH_3)(C_2H_5)_2C_3B_2(C_2H_5)_2$, a pentagonal pyramid with the metal in the apex, and green, paramagnetic $(\eta^5\text{-}C_5H_5)_2Ni_2(CH_3)(C_2H_5)_2C_3B_2(C_2H_5)_2$

(*81*). A pyramidal cobalt complex, $(CO)_3Co(CH_3)(C_2H_5)_2C_3B_2(C_2H_5)_2$, has been obtained with $HCo(CO)_4$ or $Co_2(CO)_8$ reagents (*80*).

B. Four-Carbon Carboranes

Pyramidal $C_4B_2H_6$, a 16-electron ($2n + 4$) nido cage system (Fig. 4e), was first prepared, in peralkylated form, by treatment of 1,2-bis-(diethylboryl)-1,2-dialkylethylene with a trace of $(C_2H_5)_2BCl$ at 40°C (*2*). Other alkyl derivatives have been obtained by the reaction of 1,1′-dimethyl-3-diethylboryl-4-ethyl-1-stannacyclopentadiene with CH_3-BBr_2 (*1*). The parent $C_4B_2H_6$ was first synthesized (*70*) by pyrolysis of tetramethylene diborane, $(CH_2)_4B_2H_4$, at 550°C, and later by insertion of acetylene into the small *nido*-carborane $C_2B_3H_7$ (*63*). No metal derivatives of the $C_4B_2H_6$ system had been reported by the time of this writing, but a microwave study of the parent molecule (*72*) established the pyramidal cage structure and revealed that the three C—C distances are equal (1.43 Å), supporting an electron-delocalized model of the framework bonding.

A different tetracarbon system, $(CH_3)_4C_4B_4H_4$, has been obtained by reaction of dimethylacetylene with the *nido*-ferraborane 1-$(CO)_3$-FeB_4H_8 (*12*). An intermediate in this synthesis is an apparent *closo*-ferracarborane, $(CO)_3Fe(CH_3)_4C_4B_4H_4$. Possible structures for $(CH_3)_4$-$C_4B_4H_4$ and the iron complex, based on NMR observations, are shown in Fig. 8; in both cases the proposed geometry is in accord with the electron-counting rules outlined previously. A different C_4B_4 species, $(C_2H_5)_4C_4B_4(CH_3)_4$, has been prepared by treatment of thiadiborolene, $(C_2H_5)_2C_2(CH_3)_2B_2S$, with potassium metal in THF (*82*). In this

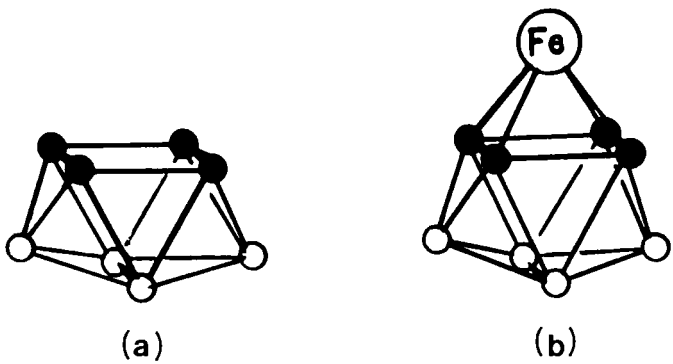

FIG. 8. Proposed structures for (a) $(CH_3)_4C_4B_4H_4$ and (b) $(CO)_3Fe(CH_3)_4C_4B_4H_4$ (*12*). ○, BH; ●, CCH_3.

compound the NMR spectra exhibit two ethyl resonances, showing that the skeletal carbon atoms are present in nonequivalent pairs; thus the cage structure of this derivative cannot be that of Fig. 8a.

At this writing the geometry of these 8-vertex carboranes is an unresolved problem. However, a closely related cobaltacarborane, $(\eta^5\text{-}C_5H_5)Co(C_6H_5)_4C_4B_3H_3$, has been prepared (*92*) and characterized by X-ray diffraction [(*93*); Fig. 9]. This material was obtained in very small quantity by the reaction of B_5H_9, cyclopentadiene, $(C_6H_5)_2C_2$, and cobalt vapor, which also generated dicarbon cobaltacarborane products. The observed geometry is essentially an arachno cage, resembling a 10-vertex closo polyhedron with two missing vertices; this is a more open structure than the nido geometry expected for a $(2n + 4)$-electron system, but it may be a consequence of severe steric repulsion by the four phenyl groups. It is also interesting that the framework C—C bond adjacent to cobalt is significantly shorter [1.379(5) Å] than the other C—C interaction [1.419(5) Å], suggesting that localized carbon–carbon bonding may be important in dictating cluster geometry. Such local effects are dominant features in the large tetracarbon clusters discussed later.

A number of four-carbon metallacarborane clusters have been prepared from derivatives of the cyclic borole system, especially pentaphenylborole, $(C_6H_5)_5C_4B$. Reactions of this compound with $Fe_2(CO)_9$ or $Ni(CO)_4$ yield $(CO)_3Fe(C_6H_5)_5C_4B$ and $(CO)_2Ni(C_6H_5)_5C_4B$, respectively; both species are *nido*-MC_4B pentagonal pyramidal systems with

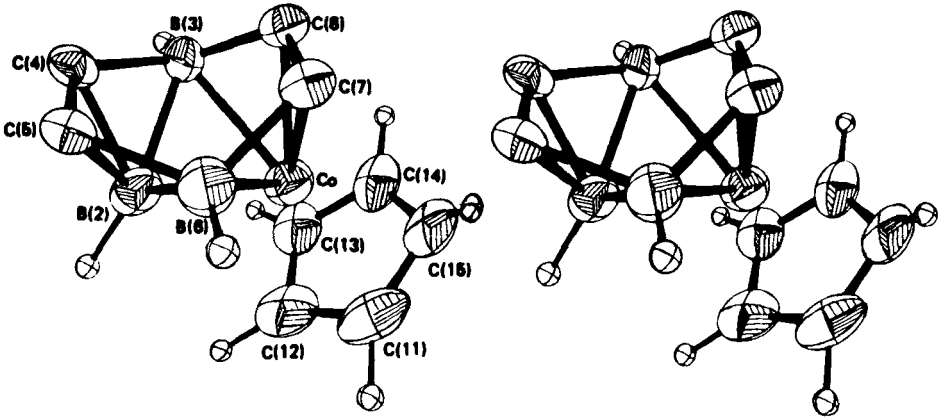

FIG. 9. Stereoview of the structure of $(\eta^5\text{-}C_5H_5)Co(C_6H_5)_4C_4B_3H_3$ (*93*). Phenyl rings are not shown. Reprinted from *Inorg. Chem.* **19**, 3650. Copyright 1980 American Chemical Society.

the metal in the apex position (*34*). Metal–borole complexes have also been obtained from 1-phenyl-4,5-dihydroborepin, a seven-membered boron heterocycle (*34*). Both monometallic (nido) complexes and dimetallic (closo) species have been characterized; an example of the latter is the dimanganese complex 1,7,2,3,4,5-$(CO)_6Mn_2C_4BH_3$-2-C_2H_5-6-C_6H_5, a pentagonal bipyramid with both apices occupied by $Mn(CO)_3$ units (*33*). Still other four-carbon metal complexes have been generated from 1,4-difluoro-1,4-diboracyclohexadiene ($F_2B_2C_4H_4$) derivatives. The cyclic planar $F_2B_2C_4R_4$ species (*85*), with the BF groups occupying para positions in a 2,5-hexadiene-like ring, is *formally* a *B,B'*-difluoro-substituted derivative of the *nido*-carborane $C_4B_2H_6$ mentioned previously (Fig. 4e); that the difluoro derivatives adopt a planar geometry testifies to the considerable influence of electron-rich ligands such as fluorine or ferrocenyl on the skeletal structure (*5*). The planar $F_2B_2C_4(CH_3)_4$ molecule readily forms sandwich complexes such as $[F_2B_2C_4(CH_3)_4]_2Ni$ (*48*), which could be considered metallacarboranes in a broad sense. The closely related 1,4-dimethyl-1,4-diborabenzene ligand, $(CH_3)_2B_2C_4H_4$, also generates sandwich complexes with cobalt and rhodium (*35, 36*).

Still other boron-containing heterocycles capable of coordination to metals are known, (e.g., derivatives of borabenzene, C_5H_5B), and a number of transition metal complexes have been characterized. Such compounds are better described as arene–metal sandwiches rather than cage compounds and are outside the scope of the present chapter, but they have been reviewed elsewhere (*23, 80*).

IV. Large Carbon-Rich Carboranes: Synthesis and Stereochemistry

A. Formation of C_4B_8 Cages via Oxidative Fusion

1. Background

The concept of constructing large cages by low-energy, metal-promoted, face-to-face fusion of smaller cages does not seem to have occurred to anyone prior to its discovery in 1974 (*53*). The principle of oxidative *coupling* to give dimeric products involving single-bond linkages has been well established for some time; processes such as the conversion of polyhedral $B_{10}H_{10}^{2-}$ to $(B_{10}H_9)_2^{2-}$ (*6, 32, 42, 62*) or of $C_2B_9H_{12}^-$ to $(C_2B_9H_{11})_2$ (*41, 78*) require an oxidant but do not involve metal-complex formation. On the other hand, the formation of the bis(carborane) 5,5'-$[(CH_3)_2C_2B_4H_5]_2$ by thermal ejection of mercury

from μ,μ'-$[(CH_3)_2C_2B_4H_5]_2Hg$ (*37*) can be described as a metal-promoted synthesis. All these processes, however, involve linkage of polyhedra rather than fusion into a single cage framework.

The oxidative fusion reaction has been shown to occur with a variety of carborane and metallacarborane species (*18, 39, 52, 54, 58, 75, 76, 91*), but the principal work (and the original discovery) utilized C,C'-disubstituted derivatives of *nido*-2,3-$C_2B_4H_8$ (Fig. 4c). The $R_2C_2B_4H_6$ species are now accessible in bench (multigram) quantities via the base-promoted addition of an alkyne to B_5H_9 (*38*).

$$B_5H_9 + RC{\equiv}CR \xrightarrow[0\text{–}25°C]{Et_3N} 2,3\text{-}R_2C_2B_4H_6 + Et_3NBH_3$$

$$R = CH_3, C_2H_5, C_3H_7, \text{etc.}$$

This method affords the carborane product in a form easily separable by vacuum fractionation, in contrast to the original vapor-phase B_5H_9–alkyne thermal reaction (*68*), which gives complex product mixtures requiring chromatographic separation (hence limiting the scale to a few millimoles). However, for the preparation of parent $C_2B_4H_8$ the vapor-phase reaction of B_5H_9 and C_2H_2 is required.

Bridge deprotonation of $C_2B_4H_8$ and its C-substituted derivatives occurs readily in the presence of alkali-metal hydrides in ethereal solvents (*69*), giving the corresponding $R_2C_2B_4H_5^-$ anions which are versatile ligands for metal complexation and can coordinate in η^1, η^2, or η^5 fashion. Reaction with $FeCl_2$ in cold THF forms the bis(carboranyl) sandwich complex $(R_2C_2B_4H_4)_2Fe^{II}H_2$ (R = alkyl) in high yield, as shown in Fig. 10 (*52*). Similar treatment with $CoCl_2$ generates $(R_2C_2B_4H_4)_2Co^{III}H$ (*54*). Both complexes are red, air-sensitive, diamagnetic solids, which on exposure to oxygen undergo ligand fusion to form, nearly quantitatively, the colorless, air-stable carborane $R_4C_4B_8H_8$ (Fig. 10); because the ligands carry a formal −2 charge, the

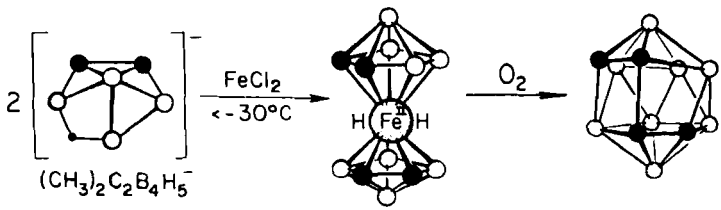

FIG. 10. Synthesis of $[(CH_3)_2C_2B_4H_4]_2FeH_2$ and conversion to $(CH_3)_4C_4B_8H_8$ via oxidative fusion (*18, 52*). ○, BH; ●, CCH_3. Reprinted from *Acc. Chem. Res.* **11**, 420. Copyright 1978 American Chemical Society.

net process involves a four-electron oxidation. Crystallographic studies of $[(CH_3)_2C_2B_4H_4]_2FeH_2$ (*75*), $(CH_3)_4C_4B_8H_8$ (*16*), and a *B*-ferrocenyl derivative of the latter species (*27*) have established the solid-state structures depicted in Figs. 11, 12, and 13, respectively. We shall return to these compounds later.

2. *Mechanism*

As this chapter is written, we are far from a detailed understanding of the fusion process. Indeed, there may well be more than one mechanism, depending on the metal, the ligand, the solvent system, or other variables. However, a number of facts have been established concerning the oxidative fusion of $(R_2C_2B_4H_4)_2FeH_2$ and $(R_2C_2B_4H_4)_2CoH$ complexes in THF (R = CH_3, C_2H_5, or C_3H_7). The process in each case is intramolecular and does not involve dissociation of $R_2C_2B_4H_4^{2-}$ ligands from the metal; thus oxidation of mixtures of $(R_2C_2B_4H_4)_2FeH_2$ and $(R'_2C_2B_4H_4)_2FeH_2$ in solution gives only $R_4C_4B_8H_8$ and $R'_4C_4B_8H_8$,

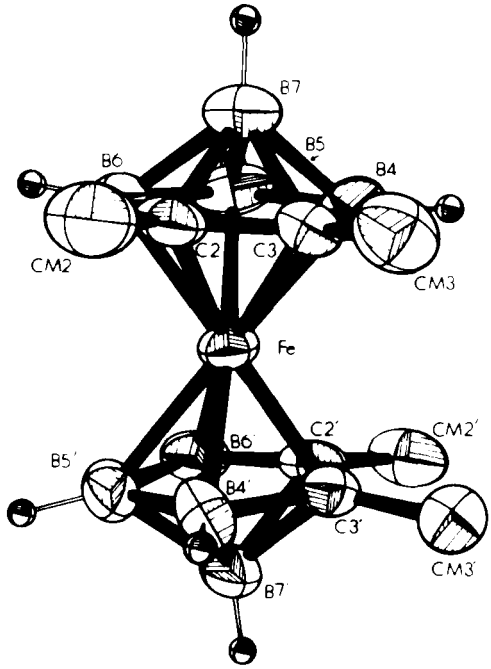

FIG. 11. Structure of $[(CH_3)_2C_2B_4H_4]_2FeH_2$ (*75*). Metal-bound hydrogen locations were not found in the X-ray study. Reprinted from *Inorg. Chem.* **18**, 263. Copyright 1979 American Chemical Society.

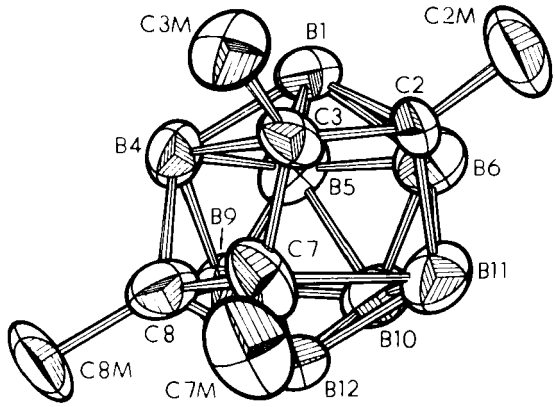

FIG. 12. Solid-state (**A** isomer) structure of $(CH_3)_4C_4B_8H_8$ (*16*) Reprinted from *Inorg. Chem.* **16**, 1847. Copyright 1977 American Chemical Society.

with no mixed-ligand ($R_2R'_2C_4B_8H_8$) products. Moreover, no ligand exchange occurs between the biscarborane metal complexes and free $R'_2C_2B_4H_5^-$ ion (*28*).

In the presence of air, the conversion to carborane occurs instantaneously in all media, but when oxygen is rigorously excluded the process is solvent dependent. No reaction occurs in diethyl ether, but in THF or dimethoxyethane (DME) an extraordinary reaction takes place almost quantitatively over several hours (*28*).

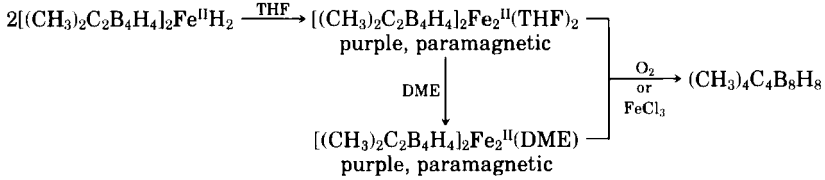

The purple diiron complex has been characterized by X-ray diffraction (as the DME adduct) and has the structure shown in Fig. 14, with an Fe—Fe distance of 2.414(4) Å (*29*). Mössbauer, ESR, and magnetic-susceptibility measurements indicate that both iron atoms are in the +2 oxidation state but that the central Fe^{2+} is low-spin d^6, while the outer Fe^{2+} is high-spin d^6, with four unpaired electrons. This reconciles nicely with a model in which the carborane ligands are more tightly bound to the central iron than to the outer metal atom; thus, the d orbitals of the outer iron are not sufficiently perturbed to produce a high-field, low-spin configuration. The purple THF and DME adducts are evidently stable under anaerobic conditions but rapidly form $(CH_3)_4C_4B_8H_8$ on exposure to air (*28*).

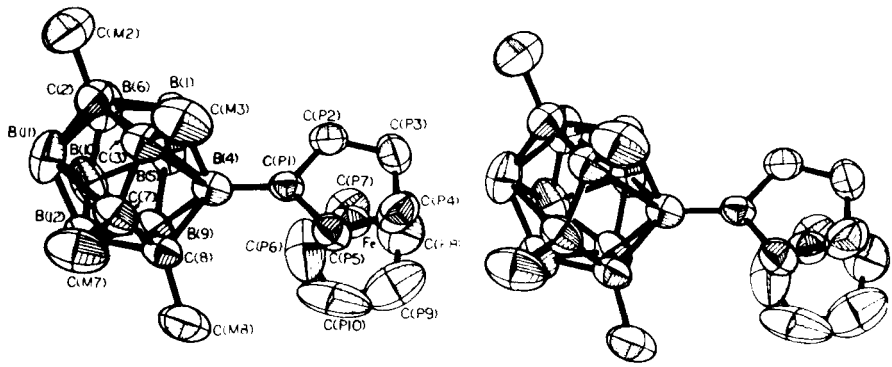

FIG. 13. Stereoview of 4-[(η^5-C_5H_5)Fe(η^5-C_5H_4)]—$(CH_3)_4C_4B_8H_7$ (*27*). Reprinted from *Inorg. Chem.* **19,** 2981. Copyright 1980 American Chemical Society.

If a catalytic quantity of $FeCl_3$ is present, the conversion of red $(R_2C_2B_4H_4)_2Fe^{II}H_2$ (R = CH_3 or C_2H_5) to the purple diiron compound occurs very quickly; an excess of $FeCl_3$ pushes the reaction all the way to $R_4C_4B_8H_8$. However, traces of Fe^{3+} (or other metal ions) may not be required to initiate the conversion, as it occurs even with $(R_2C_2B_4H_4)_2Fe^{II}H_2$ samples that have been rigorously purified by vacuum sublimation (*28*). The mechanistic details of the fusion process have not been uncovered at this writing.

Oxidative fusion appears to have significant potential as a synthetic tool, inasmuch as it has been observed with other carborane ligands and with metallacarborane substrates such as (η^5-C_5H_5)$CoR_2C_2B_4H_5^-$ (see Section V,B). Moreover, several partially fused species we have

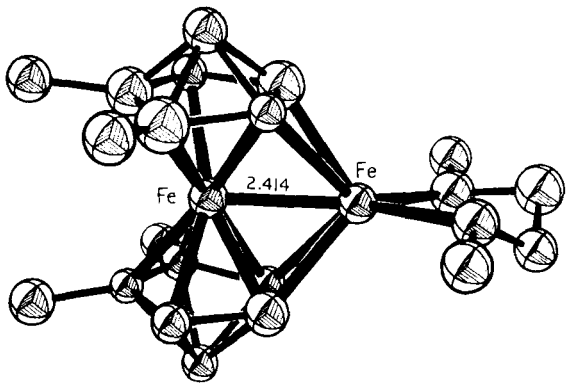

FIG. 14. Structure of $[(CH_3)_2C_2B_4H_4]_2Fe_2(OCH_3)_2C_2H_4$ (*28, 29*). Reprinted from *J. Am. Chem. Soc.* **104,** 5983. Copyright 1982 American Chemical Society.

isolated and structurally characterized may resemble early or intermediate stages in the fusion mechanism. These are discussed in Section VI.

B. Structure and Rearrangement of $R_4C_4B_8H_8$ Carboranes

The oxidative fusion of two $R_2C_2B_4H_4^{2-}$ ligands to generate $R_4C_4B_8H_8$ via metal sandwich complexes, a reaction of some interest in its own right, has led to another area of investigation, namely, the study of the $R_4C_4B_8H_8$ products. The formation of $(CH_3)_4C_4B_8H_8$ and its tetraethyl and tetrapropyl homologs occurs in high yield, and the air-stable products are easily purified by sublimation; hence it has been possible to explore in some detail the novel chemistry based on these carboranes (*18, 19*). In this subsection we outline the nonmetal stereochemistry based on the C_4B_8 system.

1. Solid-State Structure

The tetramethyl compound $(CH_3)_4C_4B_8H_8$ is an air-stable, easily sublimable, white solid (mp 138°C), which has surprising volatility at room temperature in air (in contrast, the icosahedral *o*-carborane $C_2B_{10}H_{12}$ is nonvolatile at room temperature). Its solid-state geometry (Fig. 12) has been established by X-ray crystallography, but the data are not of high quality. More recently, an X-ray study of the 4-ferrocenyl derivative (Fig. 13) confirmed, with much better precision, the same cage structure found for the unsubstituted compound; there are no significant differences in the two skeletal geometries. The C_4B_8 cage is a distorted icosahedron in which the C(2)—C(7) and C(3)—C(8) edges are stretched to nonbinding distances (~2.4 Å), thereby creating two four-sided, open faces. These stretch distortions allow all four skeletal carbon atoms to be low-coordinate, and reflect the presence of 28 (i.e., $2n + 4$) skeletal electrons, two more than a regular closo (icosahedral) cage can accommodate.

The neutral $(CH_3)_4C_4B_8H_8$ molecule is isoelectronic with the $C_2B_{10}H_{12}^{2-}$ dianions; a comparison of their structures would be of interest, but X-ray studies on the dianions have not been reported. However, the structures of two C,C′-disubstituted derivatives of the 1,2-$C_2B_{10}H_{13}^-$ monoanion (obtained by protonation of $C_2B_{10}H_{12}^{2-}$) have been determined (*7, 86*), and the cage geometry is shown in Fig. 7, type 1. This arrangement, in which one of the skeletal carbons accepts the proton and adopts a methylene-like bridging role, is clearly quite different from that of its isoelectronic C_4B_8 counterpart, shown as Fig. 7,

type 3. However, as was just noted, the structure of the nonprotonated $C_2B_{10}H_{12}^{2-}$ dianion is *not* known, and it is entirely possible that significant changes occur on protonation and deprotonation.

2. *Solution Structure*

An unusual type of fluxionality is exhibited by $R_4C_4B_8H_8$ species in solution. Boron-11 and proton pulse Fourier transform NMR studies of the tetramethyl compound in CCl_4, $CDCl_3$, benzene, and toluene (*52, 87*) reveal that a second isomer is formed in a matter of minutes, but the isomerization is only partial, and an equilibrium is established between the solid-state geometry (**A**) and the new isomer (**B**) (see Fig. 15). This behavior is largely solvent independent, and the equilibrium **B**:**A** ratio is approximately 3:5 at room temperature. When the solvent is removed the structure reverts entirely to **A**, as shown by NMR. It has not been possible to isolate the **B** form of $(CH_3)_4C_4B_8H_8$, but NMR evidence suggests a structure having a nonbonding interaction between the central carbon atoms (Fig. 7, type 2). This proposal is supported, in essence, by recent evidence on the tetraethyl carborane, $(C_2H_5)_4C_4B_8H_8$. Remarkably, this species exhibits a stereochemistry that is the *reverse* of that observed for $(CH_3)_4C_4B_8H_8$; that is, the solid-state structure corresponds to the **B** cage geometry, and an equilibrium between **B** and **A** isomers is established in solution. The direct correspondence between the **B** and **A** geometries in $(C_2H_5)_4C_4B_8H_8$ and their counterparts in $(CH_3)_4C_4B_8H_8$ is clear from the high-field ^{11}B- and ^1H- FT NMR spectra, which are closely similar (*87*). An X-ray diffraction study (*87*) has revealed the geometry of the solid-state (**B**) isomer of $(C_2H_5)_4C_4B_8H_8$ to be essentially that proposed for the **B** form of $(CH_3)_4C_4B_8H_8$, with the central carbon atoms well apart; the C(2)—C(7) and C(3)—C(8) distances are also nonbonding (~2.7 Å) so that the actual solid-state **B** structure of the $R_4C_4B_8H_8$ system (Fig. 16) is slightly more open than had been proposed.

The **A** and **B** geometries are nicely reconciled with the NMR observation of a facile, reversible interconversion in solution, because only small atomic motions are required for isomerizatin of **A** to **B** or vice versa. Moreover, the "idealized" (C_{2v}) representation of **B** (Fig. 16) is consistent with the ^1H-NMR spectrum of the **B** isomer of $(CH_3)_4C_4B_8H_8$, which indicates equivalence of all four C—CH_3 units above 40°C. Significantly, the ^1H- and ^{11}B-NMR spectra of **A** *do not* change materially at elevated temperature (*52, 87*).

Figure 16 depicts the proposed rearrangement equilibria for the $(CH_3)_4C_4B_8H_8$ isomers (*30*). Structure **C** is a cube-octahedron, a geome-

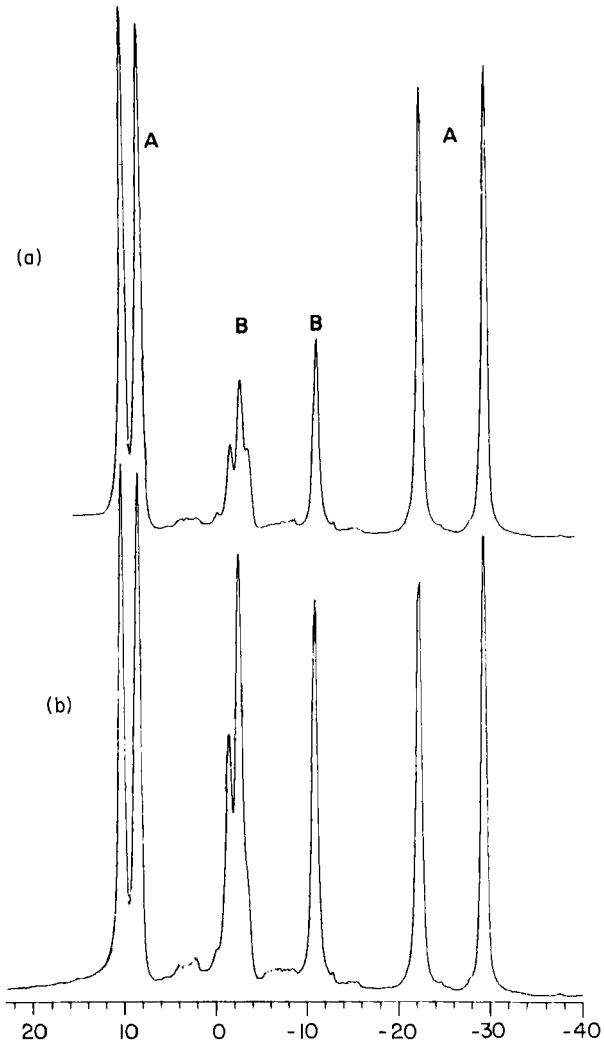

FIG. 15. 115-MHz ^{11}B- FT NMR spectra (proton decoupled) of $(CH_3)_4C_4B_8H_8$ in $CDCl_3$ solution at 25°C. (a) 2 min after dissolving. Peaks A are due to isomer **A** (solid-state structure, Fig. 12); peaks B are due to **B.** (b) Equilibrium mixture of **A** and **B,** observed 1 h 35 min after dissolving. Integrated A : B area ratio is 62 : 38 (*87*). Horizontal scale is chemical shift in parts per million [$BF_3 \cdot O(C_2H_5)_2$ = zero].

try that has been suggested as an intermediate in the isomerization of icosahedral $C_2B_{10}H_{12}$ carboranes (*47*). If **C** represents a time-averaged cage geometry for isomer **B** at 50°C, the C—CH_3 groups would be equivalent, as observed (*30*).

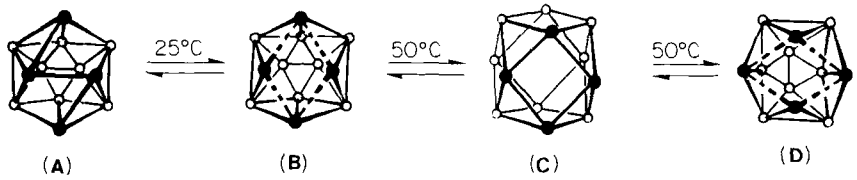

FIG. 16. Proposed fluxional interconversion of $(CH_3)_4C_4B_8H_8$ isomers **A** and **B**, showing postulated reversible thermal rearrangement of **B** at 50°C; **C** is a time-averaged (cube-octahedral) structure (*30*).

C. Formation and Fluxional Behavior of the $R_4C_4B_8H_8^{2-}$ Ion

If neutral $R_4C_4B_8H_8$, a 28-electron nido system, is reduced to the $R_4C_4B_8H_8^{2-}$ dianion, a 30-electron arachno species, one expects the cage structure to open significantly. This does in fact happen, but the stereochemistry is complex, and there seems to be no single preferred cage geometry. Treatment of $(CH_3)_4C_4B_8H_8$ with sodium naphthalenide in THF gives initially a green solution that changes to wine red and finally to yellow; presumably, the wine-colored species is a monoanion intermediate, $(CH_3)_4C_4B_8H_8^-$. The sodium salt of the yellow dianion $(CH_3)_4C_4B_8H_8^{2-}$ exhibits four equal-area ^{11}B-NMR resonances, suggesting C_s or C_2 symmetry (*50*), but the structure has not been established. However, the interaction of the dianion with transition-metal reagents generates an almost bewildering variety of metallacarborane complexes, strongly implying that the dianion exists in solution as a mixture of isomers.

An important clue to the structure of the dianion has been obtained via an X-ray diffraction study (*30*) of a *B*-cobaltocenium derivative of the $(CH_3)_4C_4B_8H_9^-$ monoanion, a species formed on protonation of $(CH_3)_4C_4B_8H_8^{2-}$. This compound, formulated as a σ-$[(C_5H_5)Co(C_5H_4)]^+$—$[(CH_3)_4C_4B_8H_8]^-$ zwitterion, has the structure shown in Fig. 17, in which the "extra" proton is located on one of the framework carbon atoms, which is lifted out of the cage skeleton and adopts a methylenic bridging role. The H—C—CH_3 bridging group is oriented such that the methyl group is located over the open face of the cage and the hydrogen is directed outward. This is reminiscent of the $R_2C_2B_{10}H_{11}^-$ structures shown in Fig. 7, type 1, except that in the latter the orientation of the R—C—H group is reversed; also, in the $R_2C_2B_{10}H_{11}^-$ structures, the bridging carbon spans a *bonded* B—B edge, whereas in the tetracarbon system the bridging carbon connects *nonbonded* boron and carbon atoms (Fig. 17). (It should be remembered, in comparing these species, that $R_2C_2B_{10}H_{11}^-$ is a 28-electron

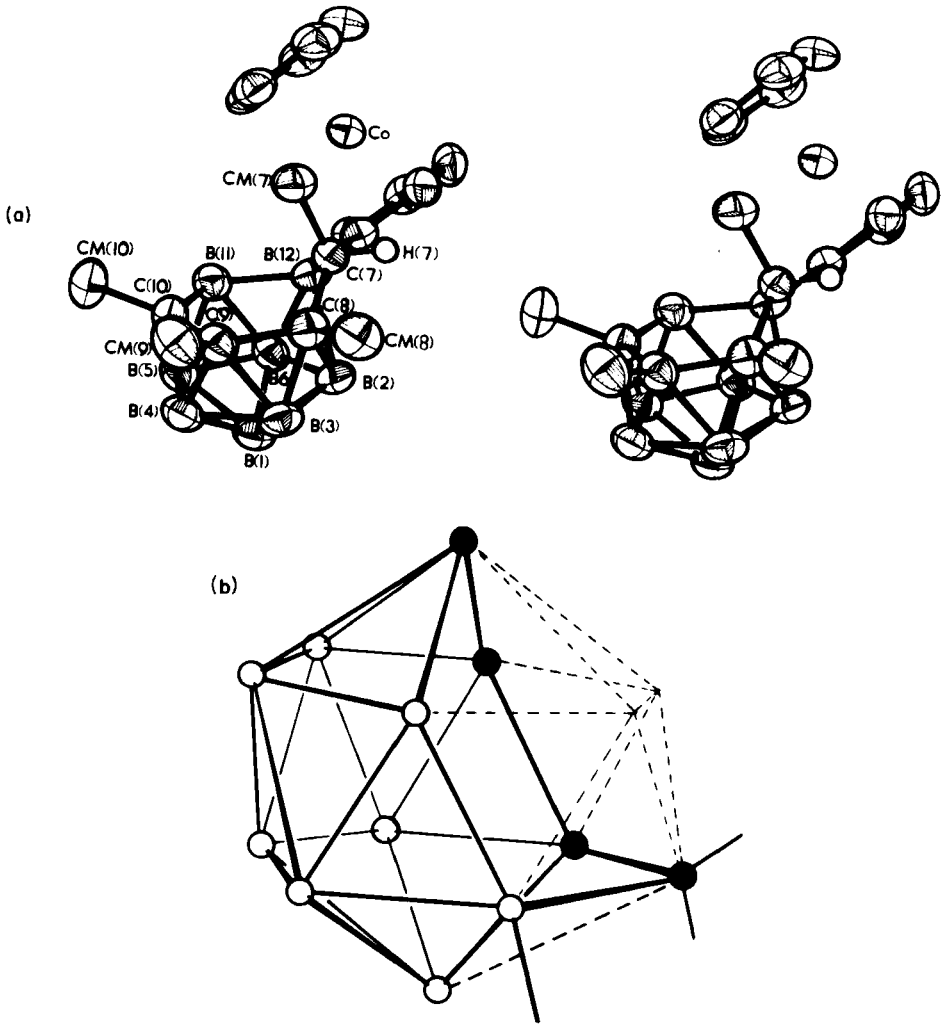

FIG. 17. (a) Stereoview of the 12-cobaltocenium derivative of the $(CH_3)_4C_4B_8H_9^-$ ion (*30*). Hydrogen atoms are omitted except for the unique methylenic hydrogen, H(7). (b) Cage structure of the cobaltocenium carborane, depicted as a fragment of a 14-vertex closo polyhedron (missing "vertices" are shown by dashed lines (*30*). Reprinted from *J. Am. Chem. Soc.* **101**, 4172. Copyright 1979 American Chemical Society.

system, whereas $R_4C_4B_8H_8^{2-}$ and its protonated form are 30-electron cages.)

The formation of $(CH_3)_4C_4B_8H_8^{2-}$ and its protonation to $(CH_3)_4$-$C_4B_8H_9^-$ are depicted in Fig. 18. The structure shown for the

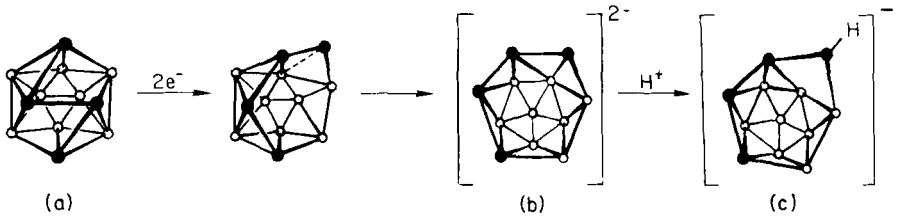

FIG. 18. Proposed scheme for conversion of neutral $(CH_3)_4C_4B_8H_8$ (a) to the $(CH_3)_4C_4B_8H_8^{2-}$ dianion (b) and the $(CH_3)_4C_4B_8H_9^-$ monoanion (c) (*30*).

dianion can be inferred from the known geometry of the monoanion (protonated species) in Fig. 17. In the absence of the extra proton, all four skeletal carbons are assumed to be fully incorporated into the cage, as shown for the dianion in Fig. 18; on protonation the unique low-coordinate carbon atom assumes an sp^3-hybridized bridging function across the open face. Protonation at carbon, rather than at the boron–boron edge on the open face, permits the cage to approach closely icosahedral-fragment geometry and relieves valence angle strain on the bridging carbon.

As mentioned previously, the $(CH_3)_4C_4B_8H_8^{2-}$ dianion gives every indication of being fluxional in solution at room temperature. Direct study of this behavior has been precluded by low solubility of salts of the dianion at low temperatures, but the established structures of transition metal complexes of the dianion provide some useful evidence. If we assume that (1) the attack of transition metal ions on a carborane anion occurs only at an open face and that (2) extensive skeletal rearrangement of metallacarborane products does not occur under the conditions of formation (i.e., room temperature), then the abundance of structural isomers obtained on metal complexation is explainable only in terms of the presence of several different isomers of the $(CH_3)_4C_4B_8H_8^{2-}$ ion in solution. Using the structure of $(CH_3)_4$-$C_4B_8H_8^{2-}$ in Fig. 18 as a model, we have proposed (*30*) that two kinds of reversible processes occur in this system, shown in Fig. 19. In the "fold-out" rearrangement, an atom on the four-membered open face of neutral $(CH_3)_4C_4B_8H_8$ is envisioned as moving away from two of its neighboring atoms, thereby creating an enlarged open face; in Fig. 19, the C—CH_3 unit at position 7 migrates in this fashion and adopts a lower-coordinate vertex on a six-membered C_4B_2 open face (structure **1A**). However, by small atomic motions, for example, stretching the B(2)—B(12) bond and compressing the C(7)—B(6) distance, B(12) can be made to occupy the unique low-coordinate position as in **1B**.

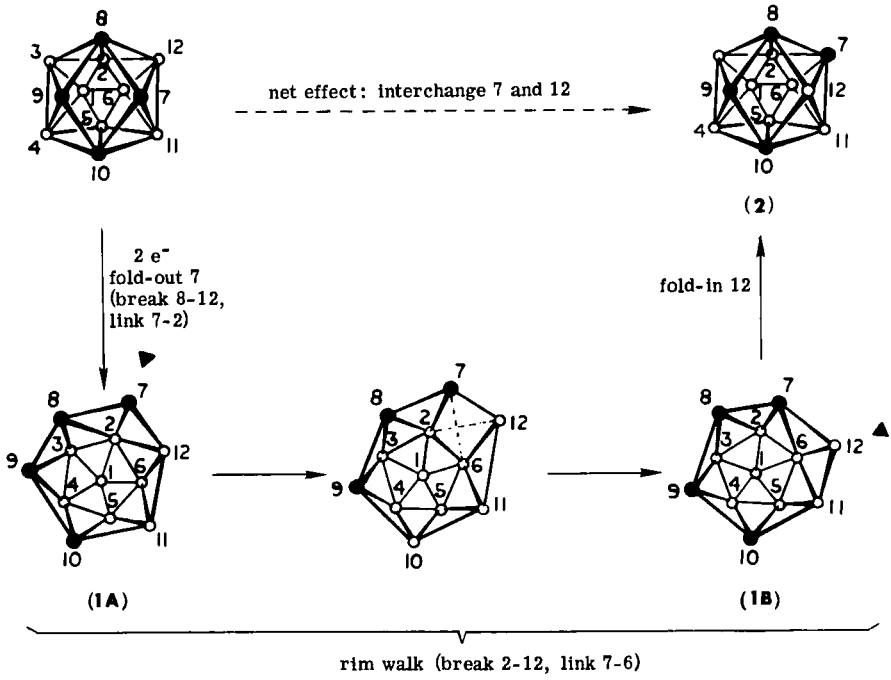

FIG. 19. Proposed scheme for fluxional rearrangement of $(CH_3)_4C_4B_8H_8^{2-}$ framework (*30*). **1A** corresponds to the established cage structure of the derivative shown in Fig. 17a; **1B** has the same geometric shape, but the unique low-coordinate vertex (marked by wedges in each structure) is now occupied by a BH unit. Reprinted from *J. Am. Chem. Soc.* **101**, 4172. Copyright 1979 American Chemical Society.

Clearly, one can in principle conduct the same kind of operation again with respect to B(12) and B(11), thus converting B(11) to a low-coordinate vertex; by extension of this idea, all six atoms on the open rim can, in turn, assume the low-coordinate role. We have labeled this kind of fluxional movement *rim walking* (*30*).

The reverse of the fold-out process depicted at the left of Fig. 19 is, of course, the fold-in, in which the low-coordinate atom (whatever it happens to be) migrates back into the open face to recreate a quasi-icosahedral cage geometry. This is illustrated at the right of Fig. 19, where B(12) is folded in to form bonds with C(8) and C(10) and produce a C(8)—C(9)—C(10)—B(12) open face (**2**). The interesting thing about the geometry of **2** is that it is related to the original geometry (upper left corner) *by interchange of C(7) and B(12)*. Obviously, one could, by a similar sequence, interchange C(7) with B(11), C(9) with B(3), or C(9)

with B(4). Even more generally, because a quasi-icosahedral geometry like that of $(CH_3)_4C_4B_8H_8$ can in principle be achieved by simply stretching *any* of the 30 edges of the icosahedron, it is clear that the fold-out → rim walk → fold-in sequence can, in theory, be used to interchange any two adjacent atoms on the 12-vertex polyhedral surface.

Actually, the preference of carbon for low-coordinate vertices, a well-established principle in carborane chemistry (*90*), is such that C—C and C—B edges are much more likely to be stretched than are the B—B interactions. (Indeed, this is shown by the fact that only two isomers of neutral $R_4C_4B_8H_8$, both involving stretch–distortion along C—C edges, are observed.) Thus the number of $(CH_3)_4C_4B_8H_8^{2-}$ isomers present in significant concentration is likely to be quite limited. Even so, the existence of several different forms of the dianion in fluxional equilibrium sets the stage for a stereochemically complicated interaction with transition-metal ions. This postulated fluxionality provides a reasonable explanation for the observed geometries of metal complexes derived from the $(CH_3)_4C_4B_8H_8^{2-}$ ion, as described in Section V.

Why are neutral $R_4C_4B_8H_8$ and $R_4C_4B_8H_8^{2-}$ ions fluxional in solution? This is a fair question because no such behavior is observed with the icosahedral $C_2B_{10}H_{12}$ isomers, and it is relatively unusual among carboranes in general. A qualitative answer is that there are opposing driving forces, one favoring icosahedral geometry because of its high inherent symmetry and stability, the other being the "electron-rich" condition (relative to the optimal $2n + 2$ electrons for a closo system), which favors cage opening. Moreover, the different forms are accessible by minor alterations in the cage framework, so that activation energies for interconversion are apt to be quite low. In this situation there is no clearly favored geometry, and the result is a highly mobile system in which even small changes, such as replacement of CH_3 by C_2H_5 or other alkyl groups, can affect the equilibria dramatically.

D. Synthesis and Stereochemistry of $(CH_3)_4C_4B_7H_9$

One of the most important properties of the dicarbon carborane 1,2-$C_2B_{10}H_{12}$ is its reaction with Lewis bases, in which the B(6)—H [or the equivalent B(9)—H] unit is selectively removed. The "hole" thus created can be filled by a wide variety of atomic units, including nonmetals, main-group metals, and transition elements. Can the $R_4C_4B_8H_8$ systems be similarly degraded? The answer is yes, but with

unexpected consequences; once again, the chemistry exhibited by the tetracarbon species is remarkably different from that of its dicarbon cousins, opening numerous new synthetic possibilities.

Triethylamine and THF are unreactive with $(CH_3)_4C_4B_8H_8$ in the absence of air, but 95% aqueous ethanol slowly converts the compound to $(CH_3)_4C_4B_7H_9$, a white, air-stable solid (mp 190°C) in yields of 40–60% (*13*). The reaction can be represented as

$$(CH_3)_4C_4B_8H_8 + 3H_2O \rightarrow (CH_3)_4C_4B_7H_9 + B(OH)_3 + H_2$$

although this is oversimplified, because there are other products not identified. The same carborane product can be prepared by the treatment of $Na^+[(CH_3)_2C_2B_4H_5]^-$ with $FeCl_2$ in THF at room temperature [recall that at −30°C these reagents generate $(CH_3)_4C_4B_8H_8$].

The molecular structure of $(CH_3)_4C_4B_7H_9$ was elucidated from an X-ray study of its monobromo derivative, which was obtained by reaction with Br_2 in carbon disulfide over aluminum chloride (*13*). Figure 20 shows the bromo species, which contains an H—C—CH_3 unit bridging the open top of a C_3B_7 basket that is isoelectronic and isostructural with $B_{10}H_{14}$. Thus once again we see the tendency of a framework carbon atom to accept a proton and thereby adopt an exopolyhedral bridging role. In this case a B—H—B hydrogen bridge is also present, as shown.

There is no doubt that the cage structure of the 11-bromo derivative (Fig. 20) is also that of the nonbrominated compound; the ^{1}H-NMR spectra are nearly identical, and the ^{11}B spectra differ, in essence, only in the replacement of a B—H doublet by a singlet resonance due to the brominated boron atom, B(11).

The cage framework can be represented as an arachno system, that is, a 13-vertex polyhedron with two vertices removed (Fig. 20b), in accordance with the presence of 28 ($2n$ + 6) skeletal electrons. The structure can also be described as a distorted 11-vertex polyhedron in which the edges connecting the apex [C(7)] to vertices 2, 3, 9, and 10 have been stretched to nonbonding distances; this stretch distortion is also consistent with the arachno electron count. Finally, one can view the molecule as a 10-vertex $(CH_3)_3C_3B_7H_8$ system that is isoelectronic with $B_{10}H_{14}$ and bridged by an exopolyhedral $HC(CH_3)$ group, as mentioned earlier.

The acid–base chemistry of $(CH_3)_4C_4B_7H_9$ is most remarkable (*13*). On treatment with sodium hydride in THF the proton attached to the bridgehead carbon is removed to give a $(CH_3)_4C_4B_7H_8^-$ anion, the framework geometry of which is significantly changed from the neu-

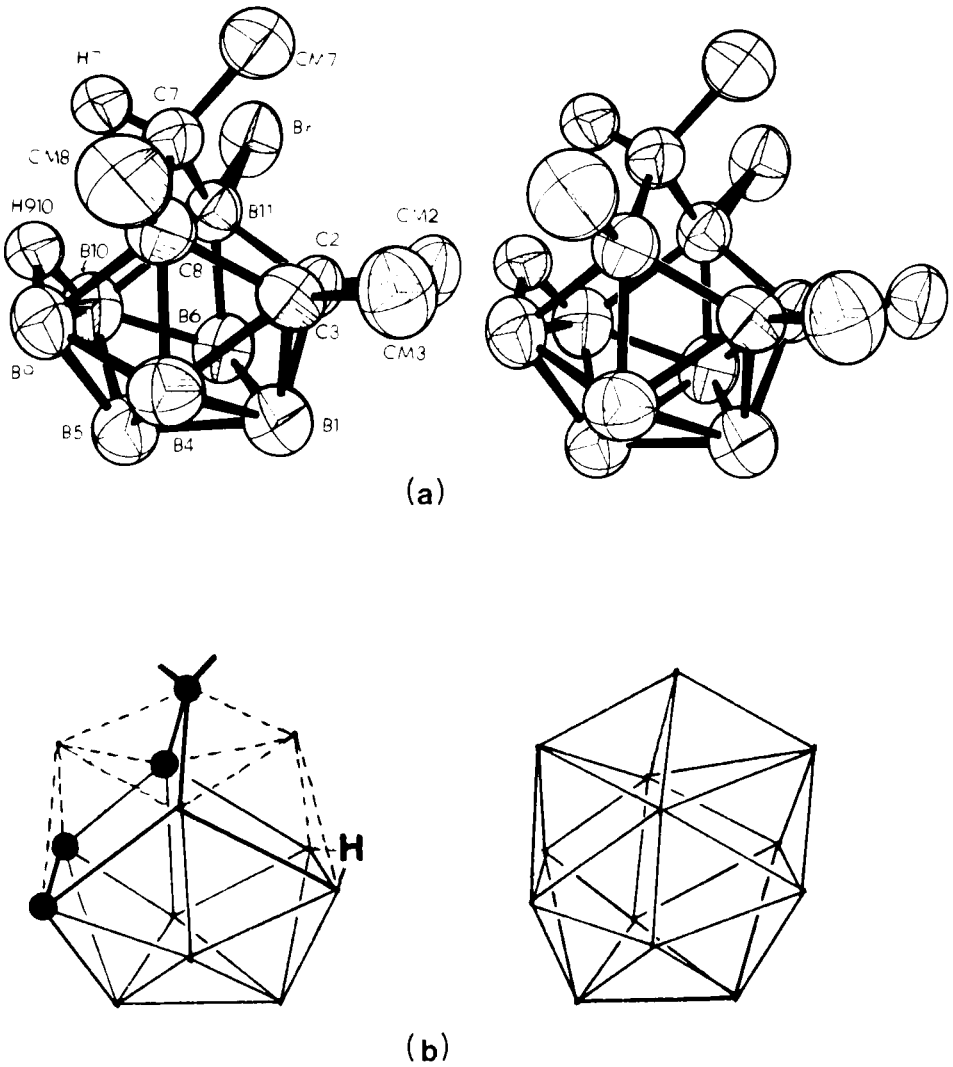

FIG. 20. (a) Stereoview of the structure of 11-Br-$(CH_3)_4C_4B_7H_8$ (*13*). (b) Same structure represented as an arachno fragment (left) of a closo 13-vertex polyhedron (right) (*13*). Reprinted from *J. Am. Chem. Soc.* **103,** 2675. Copyright 1981 American Chemical Society.

tral species, as indicated by the ^{11}B and ^{1}H spectra; reprotonation of the anion yields a neutral $(CH_3)_4C_4B_7H_9$ product that is different from both the original compound and the anion.

$$\underset{\text{Isomer I}}{(CH_3)_4C_4B_7H_9} \xrightarrow[-H_2]{NaH} Na^+[(CH_3)_4C_4B_7H_8]^- \xrightarrow{HCl} \underset{\text{Isomer II}}{(CH_3)_4C_4B_7H_9}$$

A proposed mechanism for these interconversions is given in Fig. 21. That the proton removed is H(7) rather than the bridging hydrogen, H(910), is not surprising; deprotonation of the dicarbon species $(CH_3)_2C_2B_7H_{11}$ occurs similarly (*66*), and indications in general are that bridging CH protons in carboranes are more acidic than BHB bridges.

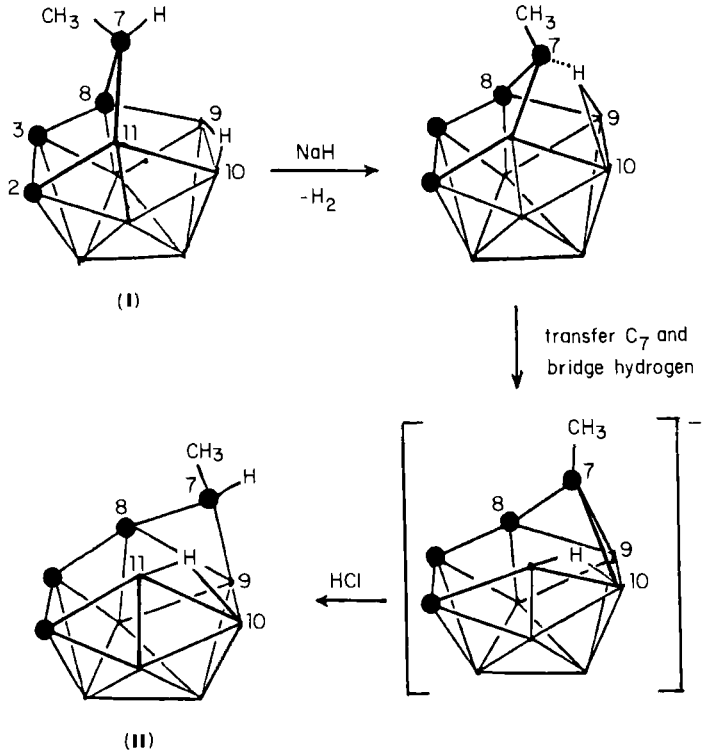

FIG. 21. Proposed scheme for conversion of $(CH_3)_4C_4B_7H_9$, isomer I, to II via deprotonation to $(CH_3)_4C_4B_7H_8^-$ and reprotonation (*13*). The structure of I is established; the others shown are based on NMR evidence. Reprinted from *J. Am. Chem. Soc.* **103**, 2675.

The structures shown in Fig. 21 for the anion and for isomer **II** have been proposed from NMR evidence combined with certain intuitive ideas about carborane rearrangements. First, removal of the CH proton from **I** obviously creates coordinative unsaturation at C(7), which can be relieved by movement of that atom into bonding interaction with B(9) and B(10); this, however, would induce the bridging hydrogen to move to a new location, very probably the B(10)—B(11) edge on the open face, as in the anion structure depicted. On reprotonation of the anion, reversion to the original structure (**I**) does *not* occur, evidently because that would entail a higher activation energy than does the conversion to **II** as shown. If the proposed geometry of **II** is correct, as is strongly indicated by the NMR spectra, it can be seen that only minor rearrangement [i.e., severing the C(7)—B(10) link and addition of a proton to C(7)] is required to convert the anion to **II**; re-formation of isomer **I**, in contrast, would require somewhat more atomic movement (including the relocation of the BHB bridge).

These processes represent, insofar as this author is aware, the first instance of carborane skeletal rearrangements induced by manipulation of protons under mild conditions. It can be assumed that other examples will be found, and this kind of stereochemistry is likely to prove quite general among carbon-rich carborane systems.

A scheme for the synthesis of $(CH_3)_4C_4B_7H_9$ (Fig. 21, **I**) from $(CH_3)_4C_4B_8H_8$ is presented in Fig. 22. The structure depicted for $(CH_3)_4C_4B_8H_8$ is that of isomer **B** (see Fig. 16), but clearly the same

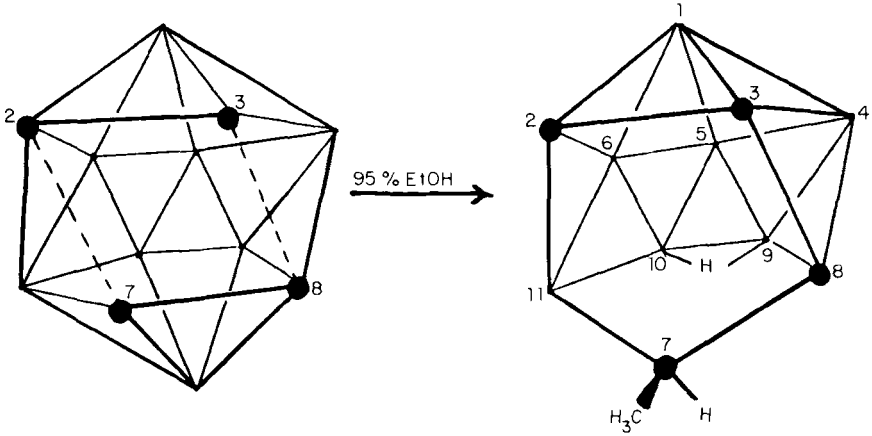

FIG. 22. Proposed scheme for conversion of $(CH_3)_4C_4B_8H_8$ to $(CH_3)_4C_4B_7H_9$ via removal of an apex BH and addition of hydrogen to C(7) (*13*). Reprinted from *J. Am. Chem. Soc.* **103**, 2675. Copyright 1981 American Chemical Society.

conversion could be drawn starting with isomer **A**. As shown, an apex BH unit is removed, atom C(7) picks up a hydrogen and moves into a bridging position [retaining its bonds to C(8) and B(11)], and a second hydrogen enters the open face as a BHB bridge between B(9) and B(10) (*13*). The attack of ethanol on B(12) is taken as evidence that this site and its equivalent, B(1), are the most electrophilic vertices in $(CH_3)_4C_4B_8H_8$; this correlates nicely with the fact that these are the only two boron atoms adjacent to more than one carbon. The well-known base degradation of 1,2-$C_2B_{10}H_{12}$ to $C_2B_9H_{12}^-$ (*21*) follows a similar pattern, in that the boron removed is vicinal to both carbon atoms and is, again, the most electrophilic site in the cage. [However, the observed bromination of $(CH_3)_4C_4B_7H_9$ at B(11), described previously, is somewhat surprising; electrophilic halogenation of the $C_2B_{10}H_{12}$ isomers usually takes place at boron atoms distant from carbon (*21*).]

V. Tetracarbon Metallacarboranes

The introduction of metals into carbon-rich carborane frameworks might be expected to produce some unusual stereochemistry, and this has amply been borne out by experience. When viewed against the known metallacarboranes based on one- and two-carbon systems (especially those derived from the $C_2B_{10}H_{12}$ isomers), the chemistry of the carbon-rich metal complexes is so different as to be almost beyond comparison; here one is well advised to "throw out the book." The basic reason for this dichotomy is that in the C_4 system the carbon atoms play a more distinctive stereochemical role and exhibit a clearly "non-boron" character.

A. Synthetic Routes

Four main pathways to four-carbon metallacarboranes have been described, namely, (1) oxidative fusion of dicarbon metallacarboranes, (2) direct insertion of metals into neutral C_4 carboranes, (3) metal insertion into C_4 carborane anions, and (4) thermal rearrangement. Of these routes, the first has no parallel in the synthesis of two-carbon metallacarboranes; methods 2, 3, and 4 are reminiscent of well-known procedures in the C_2-metallacarborane area, although for the most part the similarity is in concept only and does not hold in detail.

B. Oxidative Fusion of Dicarbon Metallacarboranes

1. Conversion of Two CoC_2B_3 Units to a $Co_2C_4B_6$ Cage

The face-to-face fusion of pyramidal $R_2C_2B_4H_4^{2-}$ ligands via metal complexation was described in Section IV,A. Metallacarborane analogs in which the apex is occupied by a metal can also undergo fusion, as shown by the conversion of 1,2,3-(η^5-C_5H_5)$CoR_2C_2B_3H_4^-$ (R = H or CH_3) ions to dicobalt, tetracarbon species (*91*).

$$2(C_5H_5)CoR_2C_2B_3H_4^- \xrightarrow[-2e^-,\ -H_2]{[O]} (C_5H_5)_2Co_2R_4C_4B_6H_6$$

R = CH_3, 1 isomer; H, 3 isomers

When R = CH_3, only one isomer of the $Co_2C_4B_6$ system is obtained, the structure of which (*76*) is shown in Fig. 23 and also in Fig. 7, type 4.

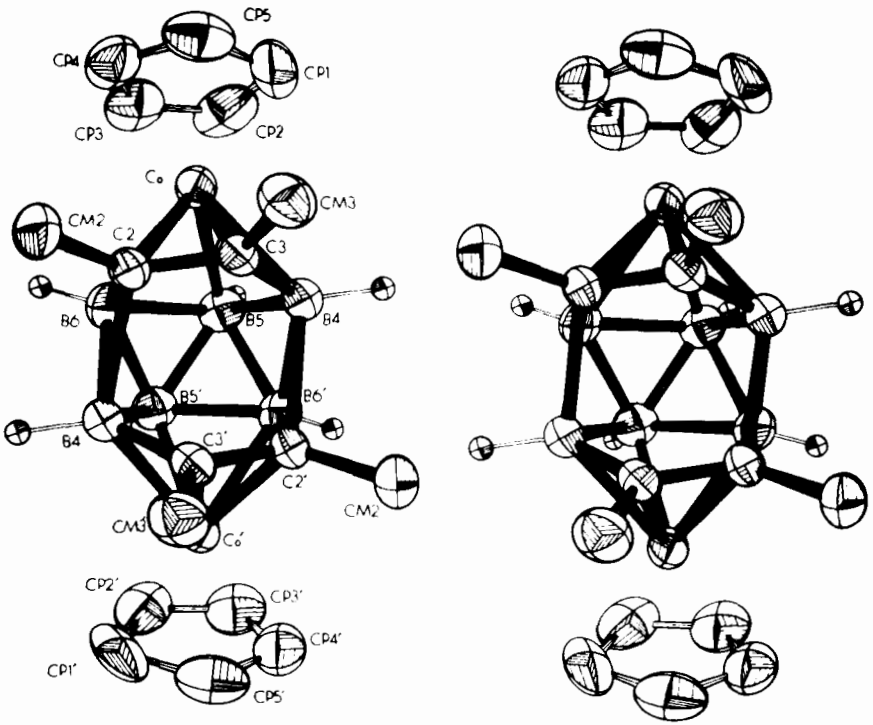

FIG. 23. Stereoview of (η^5-C_5H_5)$_2Co_2(CH_3)_4C_4B_6H_6$, isomer V (*76*). Reprinted from *Inorg. Chem.* **18**, 1936. Copyright 1979 American Chemical Society.

This complex is isoelectronic with $(CH_3)_4C_4B_8H_8$, and its cage geometry is similar except that in the dicobalt species the carbon–carbon distance across the center of the open face is distinctly nonbonding [2.791(5) Å], whereas, in the solid form (Fig. 16, **A**) of the carborane, it is bonding [1.515(5) Å] (*27*). This comparison provides a neat illustration of the electronic effects on cage structure induced by replacement of BH with $Co(C_5H_5)$ units at the apices. Evidently the metal–carbon bonding is relatively localized, tying up electron density at the expense of the central C—C interaction; in $(CH_3)_4C_4B_8H_8$ (Fig. 12) electron delocalization is more uniform and icosahedral geometry is more closely approached. [Of course, as we have seen in Section IV,B, the energy difference between the **A** and **B** forms, which, respectively, have bonded and nonbonded central carbon–carbon interactions, is quite small and leads to an **A** $\rightleftarrows$ **B** equilibrium in solution. Moreover, as noted previously, mere replacement of the four CH_3 groups in $(CH_3)_4C_4B_8H_8$ by C_2H_5 units is sufficient to reverse the situation and favor the **B** structure in the solid state (*87*).]

The structure of the dicobalt complex (Fig. 23) clearly resembles two CoC_2B_3 pyramidal units fused along the boron–boron edges and no doubt reflects a fusion process related to the formation of the $R_4C_4B_8H_8$ carboranes from $R_2C_2B_4H_4^{2-}$ pyramidal ligands (see previous discussion). When the starting material is the parent cobaltacarborane 1,2,3-$(\eta^5\text{-}C_5H_5)CoC_2B_3H_5$, not one but three $(C_5H_5)_2Co_2C_4B_6H_{10}$ isomers are obtained (*91*). One of these (designated isomer **V**) has a cage structure

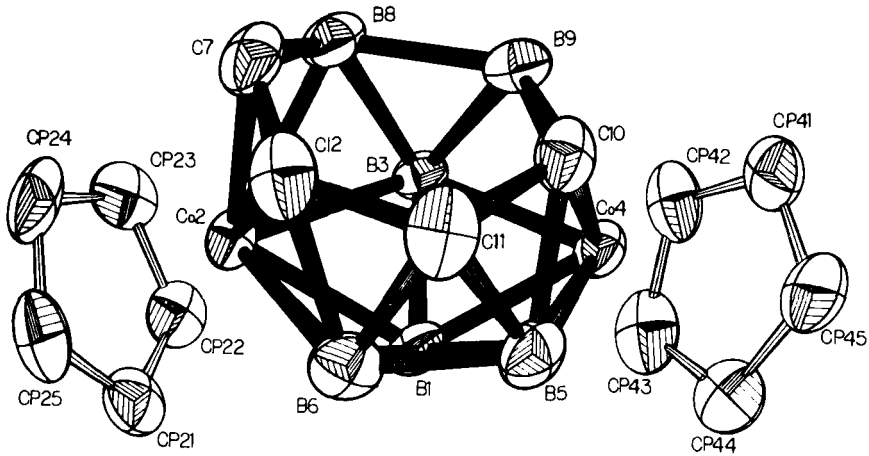

FIG. 24. Structure of $(\eta^5\text{-}C_5H_5)_2Co_2C_4B_6H_{10}$, isomer **VII** (*91*). Reprinted from *J. Am. Chem. Soc.* **100**, 5045. Copyright 1978 American Chemical Society.

analogous to that of $(C_5H_5)_2Co_2(CH_3)_4C_4B_6H_6$ in Fig. 23. A second isomer has the geometry depicted in Fig. 24, and the third, which has not yet been confirmed by X-ray data, is proposed to have pseudoicosahedral geometry. In the last instance, the high symmetry evident in both the ^{11}B- and ^1H-NMR spectra points rather strongly to this structure.

Figure 25 presents a mechanistic scheme (*76*) that accounts for all three isomers and indicates pathways for their interconversions. Species **I**, **II**, and **III** are proposed intermediates that have not been isolated, although tentative NMR evidence has been obtained for the quadruple-decker complex **I**. The formation of **I** would be analogous to the synthesis of $[(CH_3)_2C_2B_4H_4]_2CoH$ from $(CH_3)_2C_2B_4H_5^-$ and $CoCl_2$ in THF as described previously. To date, all efforts to characterize the quadruple-decker (**I**) have been unsuccessful, although an isomer of that species (in which one of the "end" cobalts is proposed to occupy an

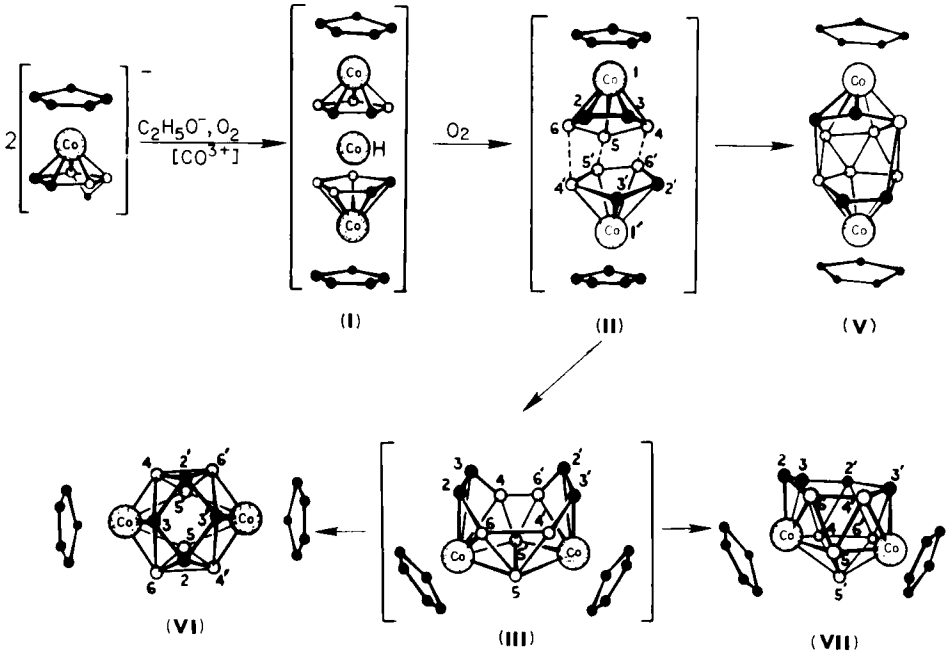

FIG. 25. Proposed scheme for formation of the three known isomers of $(\eta^5\text{-}C_5H_5)_2Co_2C_4B_6H_{10}$. Structures of **V** and **VII** are crystallographically established, and that of **VI** is postulated from NMR data; bracketed structures are possible intermediates (*76*). ○, BH; ●, CH. Reprinted from *Inorg. Chem.* **18**, 1936. Copyright 1979 American Chemical Society.

equatorial rather than an apical vertex) has been isolated (*54*). As shown, the three isomeric $(C_5H_5)_2Co_2C_4B_6H_{10}$ products **V**, **VI**, and **VII** are all postulated to originate from a common intermediate, **II**. Despite the dissimilarity of the three isomers, the atomic movements in **II** and **III** required to interchange them are relatively small.

Of the three isomers, **V**, **VI**, and **VII**, the "expected" geometry for a 28-electron 12-vertex (nido) system is represented by **VII** (Fig. 7, type 5), which is a fragment of a 13-vertex closo polyhedron. Indeed, for the analogous monocobalt system $(\eta^5\text{-}C_5H_5)Co(CH_3)_4C_4B_7H_7$, this type-5 geometry is thermodynamically favored, as demonstrated by a thermal isomerization study (see Section V,E). Presumably, **VII** is the preferred structural arrangement for the $Co_2C_4B_6$ system also, though this has not been proved. Why, then, in the fusion of the dimethyl complex $(\eta^5\text{-}C_5H_5)Co(CH_3)_2C_2B_3H_4^-$, is only one isomer (**V**) of $(\eta^5\text{-}C_5H_5)_2Co_2(CH_3)_4C_4B_6H_6$ obtained? Our reasoning is that the steric bulk of the methyl groups inhibits the close approach of C—CH_3 units in **III** (Fig. 25), as required for generation of **VII** and **VI**; the formation of **V** requires no such interaction, so that **V** is kinetically stabilized.

2. *Conversion of $[(CH_3)_2C_2B_4H_4]CoH[(CH_3)_2C_2B_3H_5]$ to $(\eta^5\text{-}C_5H_5)Co(CH_3)_4C_4B_7H_7$ (Isomer I)*

An apparent example of the oxidative fusion of C_2B_4 and C_2B_3 ligands involves the treatment of the sandwich complex $[(CH_3)_2C_2B_4H_4]CoH[(CH_3)_2C_2B_3H_5]$ with NaH or *n*-butyllithium to remove the metal-bound proton, followed by reaction of the resulting anion with $CoCl_2$ and NaC_5H_5 (*51*). The main product, $(\eta^5\text{-}C_5H_5)Co(CH_3)_4C_4B_7H_7$ (isomer **I**), has the open-cage structure depicted in Fig. 7, type 4, and it is identical to the species obtained on direct insertion of $Co(C_5H_5)$ into neutral $(CH_3)_4C_4B_8H_8$ (see following discussion). One assumes that the $[(CH_3)_2C_2B_4H_4]Co[(CH_3)_2C_2B_3H_5]^-$ anion undergoes fusion to generate a C_4B_7 carborane cage, into which cobalt is inserted to give the observed CoC_4B_7 product. However, this complex is isolated in only 14% yield, and other products are also formed, so that this reaction is not as clear-cut an example of fusion as are those involving the $[R_2C_2B_4H_4]_2MX_x$ species described previously.

C. Metal Insertion into Neutral C_4 Carboranes

Treatment of $(CH_3)_4C_4B_8H_8$ in solution with neutral metal reagents, at elevated temperature or under ultraviolet light, affords a variety of metallacarborane products (*50, 51*).

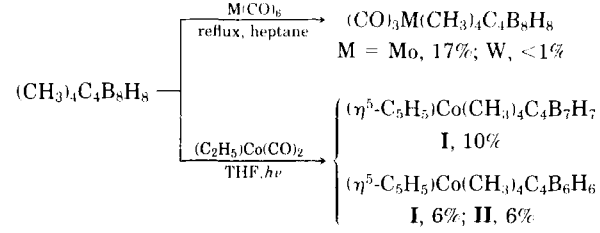

Because $(CH_3)_4C_4B_8H_8$ is fluxional and lacks a single, well-defined open face (see previous discussion), there is little steric control in such reactions; it is difficult to predict a priori the cage structures of the products, aside from the general rule in metallacarborane chemistry that metal atoms usually enter the cage in proximity to carbon atoms. The molybdenum complex (*50*) is a formal $(2n + 2)$-electron system corresponding to a 13-vertex closo polyhedron, but NMR data tell us only that the molecule lacks symmetry (no spectra are available for the tungsten species).

The cobalt reaction (*51*), however, is reasonably well defined in terms of product structures and a plausible pathway can be envisioned for their formation (Fig. 26). The major product, $(\eta^5\text{-}C_5H_5)Co(CH_3)_4C_4B_7H_7$, isomer **I**, has the type-4 structure (Fig. 7), which is directly analogous to that of $(\eta^5\text{-}C_5H_5)_2Co_2(CH_3)_4C_4B_6H_6$ (**V**), with one $Co(C_5H_5)$ unit replaced by BH. X-Ray structure determinations on both $(C_5H_5)Co(CH_3)_4C_4B_7H_7$ (*89*) and its 12-ethoxy derivative (*77*) reveal an open geometry with nonbonded C—C distances (~2.8 Å) across the open face; this is precisely like the dicobalt $Co_2C_4B_6$ (**V**) structure and different from $(CH_3)_4C_4B_8H_8$, which has a central C—C bond, as discussed earlier. Hence replacement of even one apex BH by $Co(C_5H_5)$ is sufficient to rupture the central C—C link and open the cage; the effect clearly cannot be a steric one and must be electronic in nature.

As shown in Fig. 26, the CoC_4B_7 product can be envisioned to form via displacement of an apex BH unit in the carborane reagent by $Co(C_5H_5)$. The other two characterized products in this reaction, both 11-vertex CoC_4B_6 systems, are assumed to form by loss of boron from the CoC_4B_7 species (*51*), as is also depicted in Fig. 26. The structures shown for these compounds were originally postulated from NMR data, which in both cases indicate mirror symmetry, but there was no unequivocal way to identify which was which. As it happens, X-ray diffraction studies of both compounds (*60*) have confirmed the proposed cage geometries (Fig. 27). These compounds are 11-vertex, 26-electron $(2n + 4)$ systems, which, as expected, adopt clear nido structures,

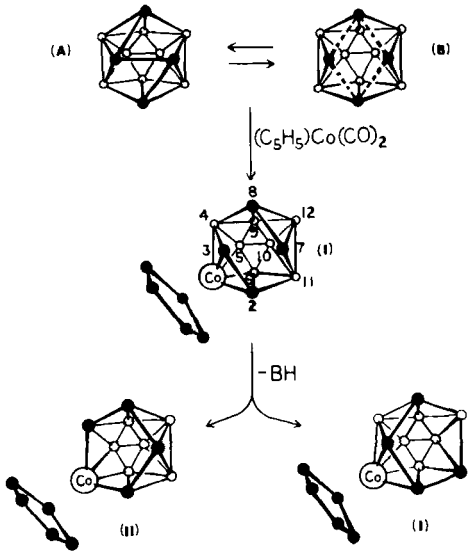

FIG. 26. Proposed scheme for formation of $(\eta^5\text{-}C_5H_5)Co(CH_3)_4C_4B_7H_7$, isomer **I**, from $(CH_3)_4C_4B_8H_8$ (**A** and **B**), and its degradation to $(\eta^5\text{-}C_5H_5)Co(CH_3)_4C_4B_6H_6$, **I** and **II** (*51*). ○, BH; ●, CH, CCH_3. Reprinted from *Inorg. Chem.* **18**, 2174. Copyright 1979 American Chemical Society.

based on removal of one vertex from an icosahedron. Unlike the 12-vertex nido systems, in which a variety of kinetically stabilized cage structures is observed, the icosahedral fragment is clearly the dominant geometry for 11-vertex, 26-electron cages.

The formation of the two CoC_4B_6 isomers from the CoC_4B_7 system as shown has not been directly established, but it does provide a straightforward explanation of their origin. Thus removal of B(11)—H from $(\eta^5\text{-}C_5H_5)Co(CH_3)_4C_4B_7H_7$, followed by movement of C(7)—CH_3 into the vacated position, yields $(\eta^5\text{-}C_5H_5)Co(CH_3)_4C_4B_6H_6$, (Fig. 26, **I**); removal of B(4)—H with similar migration of C(4)—CH_3, forms **II**. It should be noted that in both structures all four skeletal carbons occupy low-coordinate vertices on the open rim. This reflects a general trend that was mentioned in Section II and that is further discussed later in the chapter.

D. METAL INSERTION INTO $R_4C_4B_8H_8^{2-}$ DIANIONS

1. Cobalt Complexes

The reaction of transition-metal reagents with $R_4C_4B_8H_8^{2-}$ dianions furnishes another route to carbon-rich metallacarboranes. As we

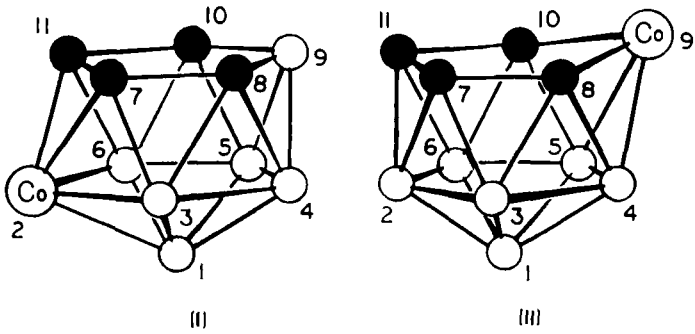

FIG. 27. Established cage geometries of $(\eta^5\text{-}C_5H_5)Co(CH_3)_4C_4B_6H_6$, isomers **I** and **II** (*60*). Reprinted from *Inorg. Chem.* **20**, 3858. Copyright 1981 American Chemical Society.

described earlier, the abundance of isomers generated from $(CH_3)_4C_4B_8H_8^{2-}$ under mild conditions strongly suggests that the dianion is fluxional in THF solution and that metal attack can occur on several isomeric forms of the substrate. The dianion is usually generated by reaction of neutral $R_4C_4B_8H_8$ (R = CH_3 or C_2H_5) with sodium naphthaleneide in cold THF, which is subsequently allowed to reach room temperature. Treatment of $(CH_3)_4C_4B_8H_8^{2-}$ with $CoCl_2$ and $C_5H_5^-$ ion, followed by acidification with HCl, produces three isolable compounds in low yield (*51*).

$$(CH_3)_4C_4B_8H_8^{2-} \xrightarrow[NaC_5H_5]{CoCl_2} (\eta^5\text{-}C_5H_5)Co(CH_3)_4C_4B_8H_8 + \underset{\text{isomer II}}{(\eta^5\text{-}C_5H_5)Co(CH_3)_4C_4B_7H_7} + \sigma\text{-}[(\eta^5\text{-}C_5H_5)Co(\eta^5\text{-}C_5H_4]^+\text{—}[(CH_3]_4C_4B_8H_8]^-$$

The last two products have been structurally established from X-ray studies (*30, 31*), and the geometry of the CoC_4B_8 species has been deduced from the known structure of an NiC_4B_8 system (*31*), which appears, from NMR evidence, to be analogous to the cobalt compound. A schematic diagram of the reaction, Fig. 28 (*51*), represents two isomers of $(CH_3)_4C_4B_8H_8^{2-}$ in equilibrium; a mechanism for the interconversion of such species was suggested earlier (see Fig. 19). The introduction of a $Co(C_5H_5)$ unit into the cage, as shown (Fig. 28), gives the 13-vertex CoC_4B_8 nido complex, which in turn can lose a BH unit to produce the observed isomer **II** of a CoC_4B_7 system. Again, no direct mechanistic evidence is available; the scheme illustrated here is based on the known product structures and reasonable inferences. Thus it is not difficult to envision the $CoC_4B_8 \rightarrow CoC_4B_7$ conversion as shown, because it involves only removal of a boron and slight movement of a framework carbon atom to form a C—C link across the open face.

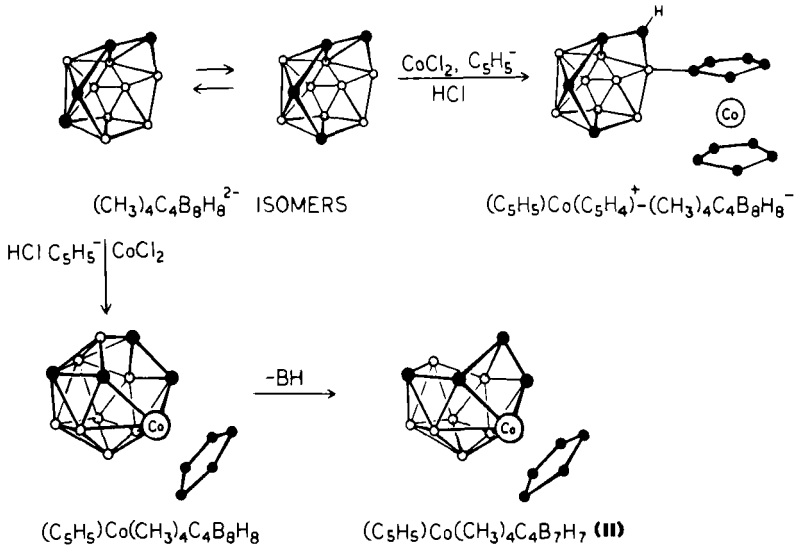

FIG. 28. Proposed scheme for reaction of $(CH_3)_4C_4B_8H_8^{2-}$ isomers with $CoCl_2$ and NaC_5H_5 in THF (*51*). The geometry depicted for $(C_5H_5)Co(CH_3)_4C_4B_8H_8$ is based on the known structure of an analogous nickel complex (see Fig. 29); the structures of the other products are established. Reprinted from *Inorg. Chem.* **18**, 2174. Copyright 1979 American Chemical Society.

The crystallographically determined structure of $(\eta^5\text{-}C_5H_5)Co(CH_3)_4C_4B_7H_7$ (**II**) (*31*), is unique and represents yet another form of nido geometry adopted by a 28-electron, 12-vertex system (Fig. 7, type 6). The central carbon–carbon bond in the framework is relatively long [1.567 (4) Å], indicating that the trans-cage bridging interaction across the open face is weak compared to normal bonds within the cage framework.

2. *Nickel Complexes*

Dichloro-1,2-bis(diphenylphosphino)ethanenickel(II) reacts with the $(CH_3)_4C_4B_8H_8^{2-}$ ion in THF to give at least five isolable nickelacarborane products, including two 12-vertex NiC_4B_7 and three 13-vertex NiC_4B_8 cage systems (*50*).

$$[(C_6H_5)_2PCH_2]_2NiCl_2 + Na_2[(CH_3)_4C_4B_8H_8] \xrightarrow[25°C]{THF} \xrightarrow{O_2} [(C_6H_5)_2PCH_2]_2Ni(CH_3)_4C_4B_7H_7 \text{ (two isomers)} + [(C_6H_5)_2PCH_2]_2Ni(CH_3)_4C_4B_8H_8 \text{ (three isomers)}$$

From ^{11}B- and ^1H-NMR observations it is evident that none of these complexes possesses a symmetry element. Because the $[(C_6H_5)_2PCH_2]_2$-

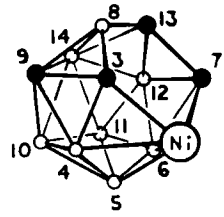

FIG. 29. Crystallographically determined cage structure of $[(C_6H_5)_2PCH_2]_2Ni(CH_3)_4C_4B_8H_8$, isomer **I** (*31*). ○, BH; ●, CCH_3. Reprinted from *Inorg. Chem.* **19**, 2087. Copyright 1980 American Chemical Society.

Ni unit is a formal two-electron donor to cage bonding [equivalent to $Co(\eta^5\text{-}C_5H_5)$ and BH], all of these species are $(2n + 4)$-electron systems of the nido class. The NiC_4B_7 isomers are 12-vertex, 28-electron cages that could well extend still further the number of distinguishable structural types in that series (see Fig. 7), but no X-ray data are available as yet. However, one of the NiC_4B_8 isomers has been characterized crystallographically (*31*), and its structure is shown in Fig. 29. This cage system can usefully be described as a 14-vertex closo polyhedron (bicapped hexagonal antiprism) from which one equatorial vertex has been removed; this geometry is clearly of the nido type and is in accord with the electron count. The well-defined five-membered open face contains three of the four carbon atoms in the cage, but this isomer is almost certainly not the thermodynamically most stable. This can be deduced from the absence of symmetry, the fact that the locations of B(8) and C(9) are reversed relative to the usual preference of carbon for low-coordinate vertices, the presence of a six-coordinate BH unit [B(14)], and the location of the metal on the open rim, where its orbital overlap with neighboring atoms would be less efficient than that of a nonrim metal atom. Thus we have yet another kinetically stabilized cage system.

The 13-vertex complex $(\eta^5\text{-}C_5H_5)Co(CH_3)_4C_4B_8H_8$ is isoelectronic with the nickel species in Fig. 29 and is believed to have the same cage geometry, although this has not been established.

3. *Iron Complexes*

The treatment of $(CH_3)_4C_4B_8H_8^{2-}$ salts with $FeCl_2$ and NaC_5H_5 in THF affords a rich harvest of isolable complexes, mostly in small yields to be sure, but air stable, characterizable, and structurally interesting (*50*).

$$(CH_3)_4C_4B_8H_8^{2-} \xrightarrow[FeCl_2]{NaC_5H_5} \xrightarrow{O_2} (\eta^5\text{-}C_5H_5)Fe(CH_3)_4C_4B_7H_8 + (\eta^5\text{-}C_5H_5)_2Fe_2(CH_3)_4C_4B_8H_8$$

I, II, III, IV

The 12-vertex FeC_4B_7 species has been characterized by X-ray diffraction (*50*), and the geometry Fig. 30, **5**) is of type 5 (Fig. 7), consisting of

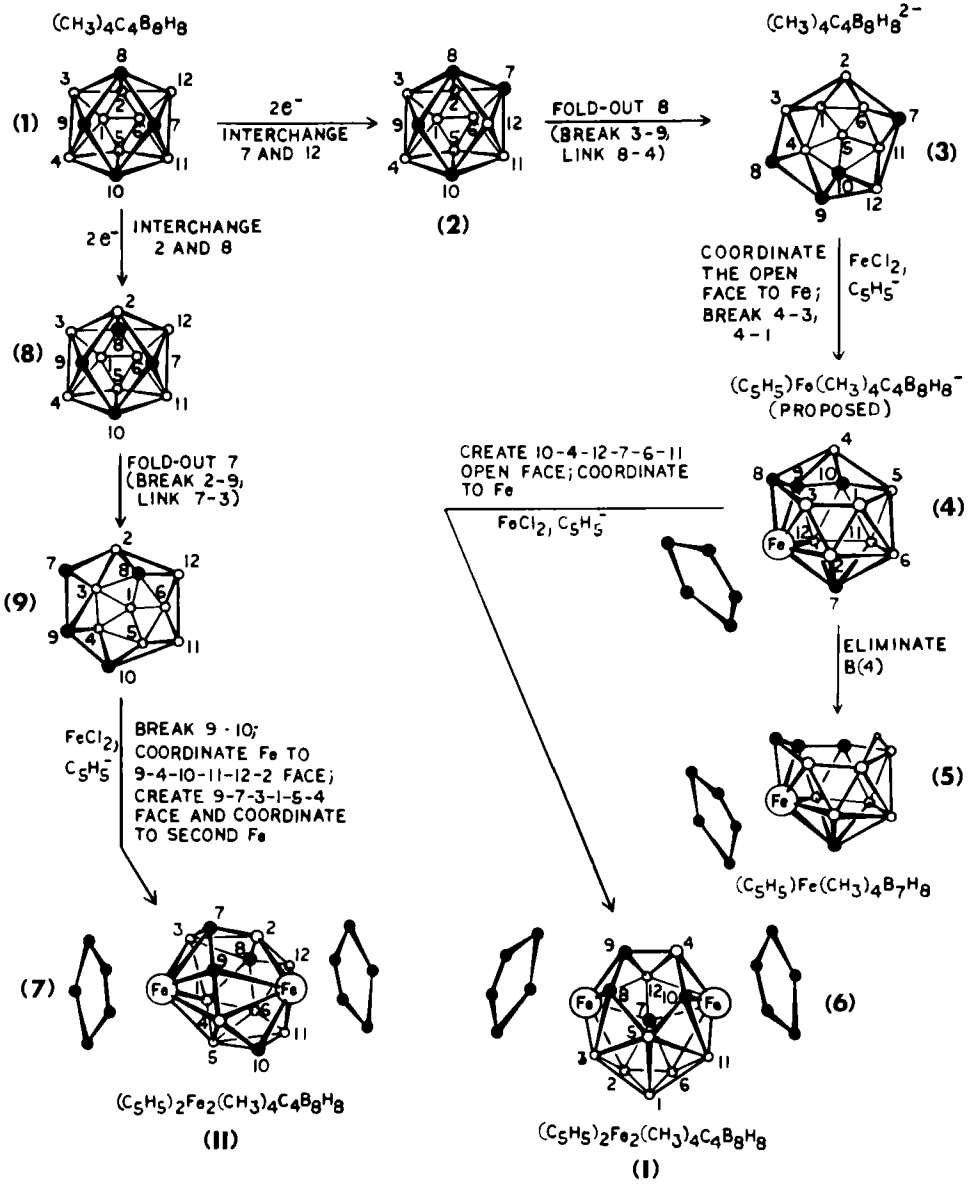

FIG. 30. Proposed sequence for formation of ferracarboranes from $(CH_3)_4C_4B_8H_8^{2-}$ isomers (*30*). ○, BH; ●, CH, CCH_3. Structures of products **5**, **6**, and **7** are established. The isomeric carborane species **2**, **3**, **8**, and **9** are proposed to form via pathways depicted in Figs. 18 and 19. Reprinted from *J. Am. Chem. Soc.* **101**, 4172. Copyright 1979 American Chemical Society.

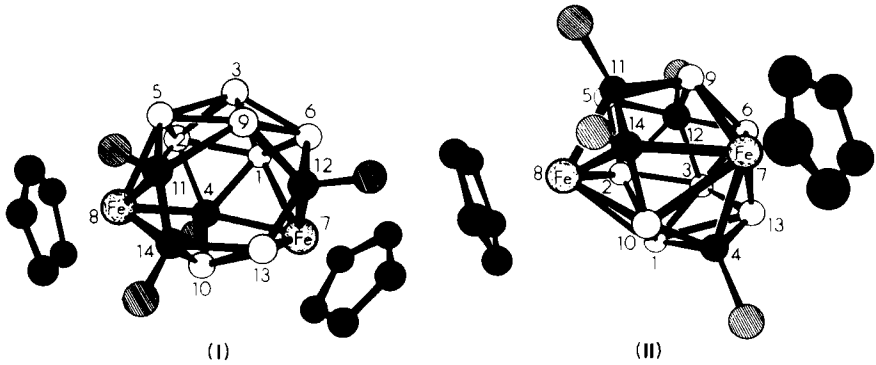

FIG. 31. Crystallographically determined structures of $(\eta^5\text{-}C_5H_5)_2Fe_2(CH_3)_4C_4B_8H_8$ isomers **I** and **II** (*57*). ○, BH; ●, C; ⊜, CH_3. Reprinted from *J. Am. Chem. Soc.* **99**, 4008. Copyright 1977 American Chemical Society.

a nido 12-vertex cage in conformity with the 28 ($2n$ + 4) skeletal electrons. The extra hydrogen atom is present in a B—H—B bridge on the open rim, as expected, but the structure has one peculiar feature: one of the skeletal carbon atoms [C(1)] is located in the apex, as far as possible from the open rim, and is not adjacent to any of the other carbons. Here again, the structure provides a clue to the mode of attack of the metal on the carborane anion substrate and further supports the idea that the $(CH_3)_4C_4B_8H_8^{2-}$ ion exists in more than one isomer in THF solution.

Figure 30 presents a mechanistic scheme that accounts for the observed geometry of $(C_5H_5)Fe(CH_3)_4C_4B_7H_8$ (**5**), as well as those of $(\eta^5\text{-}C_5H_5)_2Fe_2(CH_3)_4C_4B_8H_8$ isomers **I** and **II** (**6** and **7**, respectively, in Fig. 30). The latter two structures, determined from X-ray studies (*57*), are depicted in more detail in Fig. 31. These were among the first tetracarbon metallacarborane structures we studied, and they were astonishing at the time. Despite the closo electron count (14 vertices, 30 skeletal electrons), neither isomer has the expected closed polyhedral, bicapped square-antiprism geometry; instead, both are open-faced cages. Isomer **I** actually has a nido shape; it can be viewed as a 15-vertex closo cage with one vertex removed. That is, if one caps the open face (*56*), the resulting polyhedron has (idealized) D_{3h} symmetry, corresponding to the structure proposed by Brown and Lipscomb (*4*) for a hypothetical $B_{15}H_{15}^{2-}$ ion. In contrast, isomer **II** has a four-sided open face and bears no clear relationship to any standard polyhedron. (Indeed, if all 14 vertices were occupied by identical units there would still be no element of symmetry in the cage!)

Clearly, the structures of these 14-vertex isomers reflect their mechanism of formation from the carborane dianion. The scheme in Fig. 30 utilizes the proposed fluxional rearrangement of $(CH_3)_4C_4B_8H_8^{2-}$, as given earlier (see Fig. 19) to account for the observed ferracarborane products. It is significant that isomers **I** and **II** cannot be interconverted in a small number of steps (e.g., fewer than ten) by any simple mechanism such as diamond–square–diamond (dsd) (*47*); given that both species are obtained under mild conditions, it is obvious that they are produced independently in the reaction, together with other isomers of $(\eta^5\text{-}C_5H_5)_2Fe_2(CH_3)_4C_4B_8H_8$.

Thermal rearrangement of these 14-vertex species generates still other isomers, including, finally, the expected closo system, as described in Section V,E.

4. Chromium Complexes

Insertion of chromium into the $(C_2H_5)_4C_4B_8H_8^{2-}$ ion, utilizing $CrCl_3$ and NaC_5H_5 as reagents, forms two characterizable products, 12-vertex $(\eta^5\text{-}C_5H_5)Cr(C_2H_5)_4C_4B_7H_7$ and 13-vertex $(\eta^5\text{-}C_5H_5)Cr(C_2H_5)_4C_4B_8H_8$ (*61*). The structures of both species have been determined from X-ray crystal structure analyses (Fig. 32), and they provide further examples of "nonconformist" geometry wherein open faces seem to violate the electron-counting rules for clusters. Following the usual convention, $Cr(C_5H_5)$ is a formal (−1)-electron donor [having three fewer electrons than $Co(C_5H_5)$, a two-electron donor]; hence the two species are, respectively, 12-vertex, 25-electron and 13-vertex, 27-electron systems and are formal $(2n + 1)$-electron cages. The overall shapes of the two cages approach closo 12-and 13-vertex polyhedra, but the presence of an open face in each case is unmistakable; all transannular distances across these faces are clearly nonbinding. These structures can be rationalized as nido $(2n + 4)$-electron systems if the deficiency of three electrons is assumed to reside on chromium, which then becomes a 15-electron metal (*61*).

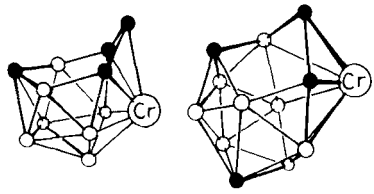

FIG. 32. Crystallographically determined cage geometries of $(\eta^5\text{-}C_5H_5)Cr(C_2H_5)_4C_4B_7H_7$ (left) and $(\eta^5\text{-}C_5H_5)Cr(C_2H_5)_4C_4B_8H_8$ (right) (*61*). ○, BH; ●, CC_2H_5.

E. Thermal Rearrangements

The numerous examples of unconventional, kinetically stabilized structures described up to this point underline the need for thermal-isomerization studies to determine the thermodynamically favored structures for these cage systems. Such studies are not trivial, because X-ray diffraction studies are usually required to establish the structures of the isomers formed; at this time only two rearrangements of tetracarbon metallacarboranes have been examined. However, in both cases some fundamental questions have been answered, and we can have confidence that the structural principles outlined in Section II do seem to hold with respect to thermodynamically preferred isomers, at least for iron and cobalt complexes.

1. The 14-Vertex $(\eta^5\text{-}C_5H_5)_2Fe_2(CH_3)_4C_4B_8H_8$ System

The unique, highly asymmetric cage structures of isomers **I** and **II** (Fig. 31) both rearrange at elevated temperature (*57*); **I** is converted to a new species, **V**, whereas **II** rearranges to another isomer (**VI**), which in turn is converted to **V**. Thus both **I** and **II** ultimately converge to the same product, **V** (Fig. 33). However, the structure of **V**, as determined crystallographically, is another open-faced cage, which in fact is closely related to its precursor **I**. Interchanging the BH and CCH_3 groups at vertices 3 and 11, respectively, *formally* converts **I** to **V** (this is not meant to imply an actual mechanism). What is the driving force for conversion of **I** to **V**? Because the overall shape of the $Fe_2C_4B_8$ cage is essentially unchanged, and because **V** actually has fewer carbons on the open face than **I**, it appears that *separation of the framework carbon atoms* is the dominant factor. This observation is in line with much previous evidence in dicarbon metallacarborane chemistry (*9, 11, 43, 64*), but the present carbon-rich systems present a much more complex stereochemical situation; there is more to consider here. Thus, when **V** itself is heated to still higher temperatures, further rearrangement takes place, yielding **VII**, as shown. This new species is believed to have a closo structure, depicted in Fig. 33, which is based on NMR evidence indicating twofold symmetry in the molecule (*57*). Although the arrangement shown, which has the carbon atoms in vertices 2, 4, 10, and 12, is only one of six possible isomers that are compatible with the NMR spectra, all six of these have at least one C—C bond, and four of them have two C—C interactions. For reasons discussed elsewhere (*57*), the 2,4,10,12-structure is preferred over the others, but this is a relatively minor point; the significant observation is that the conver-

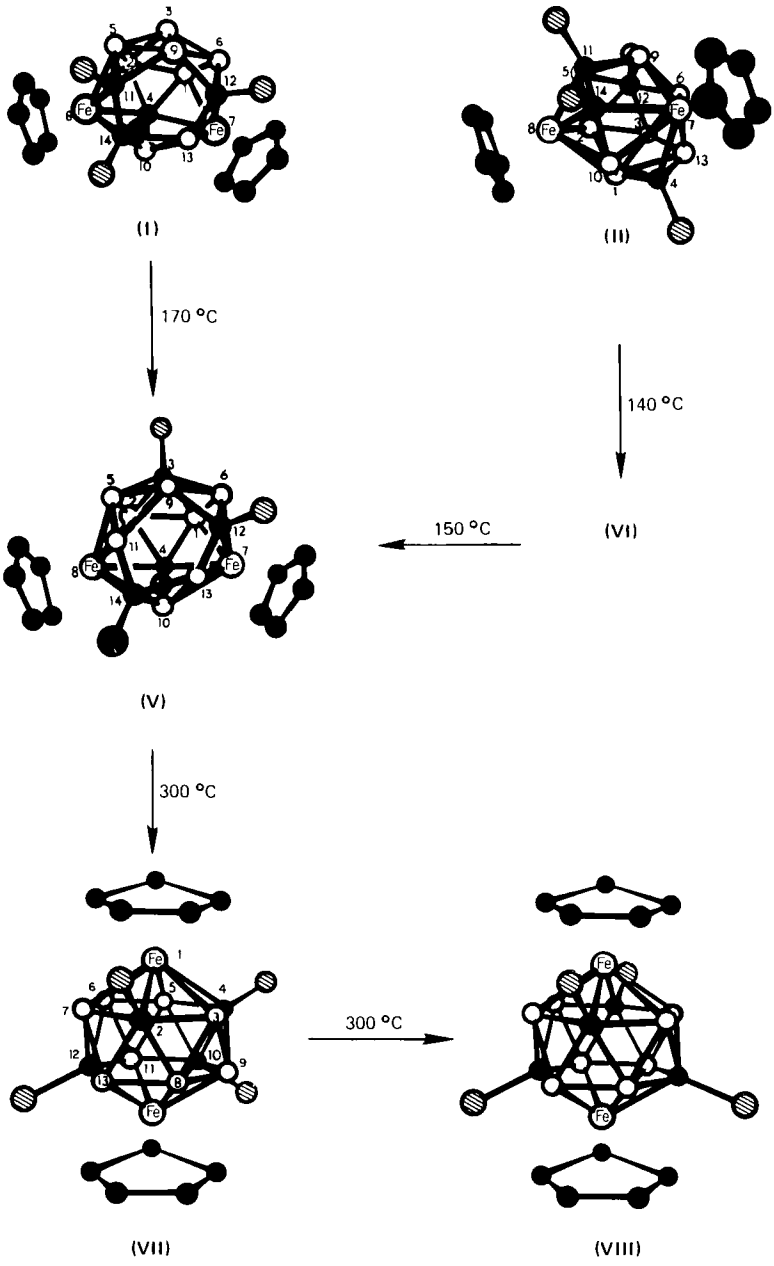

FIG. 33. Thermal rearrangement of $(\eta^5\text{-}C_5H_5)_2Fe_2(CH_3)_4C_4B_8H_8$, isomers **I** and **II**, to **V, VII,** and **VIII.** ○, BH; ●, C; ⊛, CH_3. All structures shown are crystallographically established except for **VII,** the geometry of which is postulated from NMR spectra (*57*). Reprinted from *J. Am. Chem. Soc.* **99,** 4016. Copyright 1977 American Chemical Society.

sion of **V** to **VII** involves movement of two carbon atoms toward each other, that is, to vicinal positions in the framework. Because this is contrary to the usual trend in carborane rearrangements, the lesson here must be that *the drive to achieve a closo structure is predominant.*

Continued heating at 300°C converts **VII** to the final product, isomer **VIII,** as shown (Fig. 33). The structure of **VIII** was virtually established from NMR spectra alone, which revealed the equivalence of all eight BH and all four CCH_3 units. The bicapped hexagonal-antiprism geometry with idealized D_{2d} cage symmetry was, however, established conclusively by X-ray diffraction (*73*) (Fig. 34). At this writing, this is the only crystallographically confirmed example of a 14-vertex closo system, although isomers of $(\eta^5\text{-}C_5H_5)_2Co_2C_2B_{10}H_{12}$ have been pro-

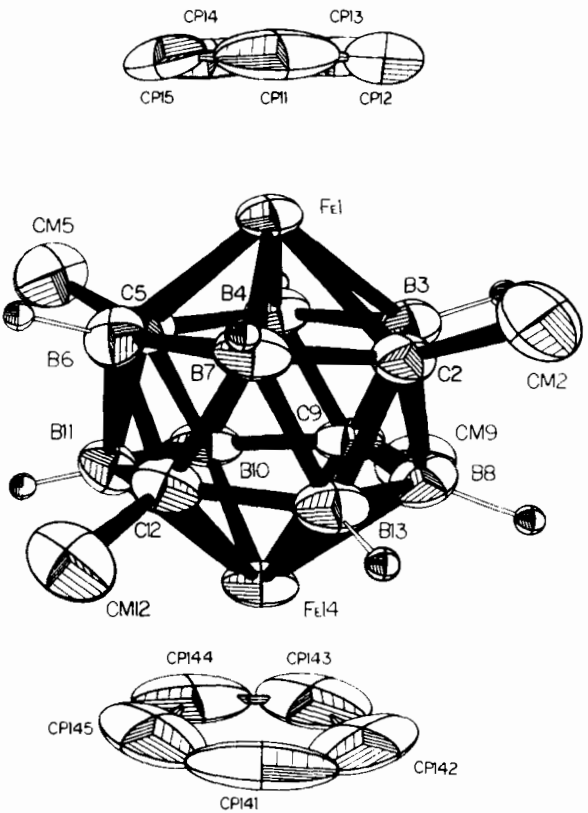

FIG. 34. Structure of $(\eta^5\text{-}C_5H_5)_2Fe_2(CH_3)_4C_4B_8H_8$ (isomer **VIII**), a 14-vertex closo polyhedron (bicapped hexagonal antiprism) (*73*). Reprinted from *Inorg. Chem.* **17,** 6. Copyright 1978 American Chemical Society.

posed to have similar structures, based on a 14-vertex closo polyhedron (*10*). The structure of **VIII** is, therefore, the preferred arrangement for the $Fe_2C_4B_8$ system and validates Wade's electron-counting rules for polyhedra of this size. If the observed rearrangement sequence in Fig. 33 can be taken to have general significance, it appears that the achievement of closo geometry (for $2n + 2$ systems) is dominant over separation of skeletal carbon atoms, which in turn is more important than placement of carbon in low-coordinate vertices. Time will tell, of course, whether these rules hold in a broader sense.

2. *The 12-Vertex* $(\eta^5\text{-}C_5H_5)Co(CH_3)_4C_4B_7H_7$ *System*

Three isomers of this $(2n + 4)$-electron complex are known, and, remarkably, all are of different structural classes, designated as types 4, 5, and 6 (Fig. 7). Thermal rearrangement of isomer **I**, which has the type-4 structure, at 140°C (*59*) gives isomer **III** (type 5), as illustrated in Fig. 35. This isomerization involves several trends: (1) adoption of a true nido geometry based on a fragment of a closo polyhedron; (2) retention of low-coordinate vertices on the rim by carbon; (3) migration of one of the carbon atoms to an isolated location on the open face; and (4) achievement of six-coordination (with respect to the cage) by the cobalt atom. The first trend is in accord with the basic ideas inherent in the closo–nido–arachno scheme described in Section II, and it also supports our intuitive feeling that the type-5 geometry is more compact and conducive to efficient delocalization of electrons than the type-4 structure of isomer **I**. (Recourse to intuition may not appeal to some, but until these systems can be handled in more definitive fashion by theorists, it can hardly be dispensed with.) Trend 2 appears to be unimportant here, because all carbons are in low-coordinate vertices in both isomers. Trend 3 illustrates the well-established tendency of cage carbon atoms to separate from each other, but it is notable here that *none of the carbons chooses to migrate away from the open face in order to achieve such separation*. This is interesting because it seems to contradict the observation of the $(\eta^5\text{-}C_5H_5)_2Fe_2(CH_3)_4C_4B_8H_8$ isomerization (**I** to **V**) discussed previously, where the conclusion was precisely the opposite. Either the two systems are sufficiently dissimilar that thermodynamic preferences of this sort are not truly comparable, or there is no low-energy pathway for migration of carbon away from the open face in the $(\eta^5\text{-}C_5H_5)Co(CH_3)_4C_4B_7H_7$ system. At present it is not possible to distinguish between these hypotheses.

Finally, as to the last point, the adoption of a high-coordinate vertex

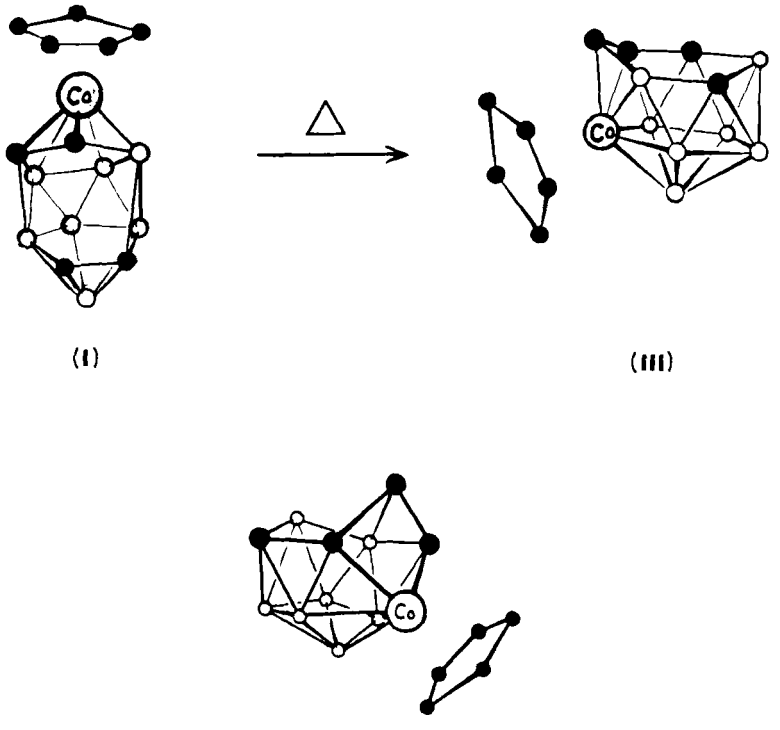

FIG. 35. Thermal rearrangement of $(\eta^5\text{-}C_5H_5)Co(CH_3)_4C_4B_7H_7$, isomer **I**, to **III** (*59*). Reprinted from *Inorg. Chem.* **20,** 1201. Copyright 1981 American Chemical Society. A third isomer, **II** (*31*), is shown below. Reprinted from *Inorg. Chem.* **19,** 2087. Copyright 1980 American Chemical Society. All three structures are established; that of **III** is evidently the thermodynamically preferred geometry.

by cobalt is in line with a general trend in cobaltacarborane and cobaltaborane chemistry; as a rule, iron and cobalt tend to maximize their coordination to the borane cage when the opportunity presents itself. It can be argued, in simple qualitative fashion, that the high-coordinate sites allow more efficient overlap between metal and framework orbitals. However, nickel and other electron-rich metals often exhibit the reverse trend, favoring low-coordinate cage vertices [for example, in the metallaboranes $(\eta^5\text{-}C_5H_5)_4M_4B_4H_4$, both of which are 8-vertex closo dodecahedra, the metal atoms occupy the high-coordinate vertices when M is cobalt (*74*), but low-coordinate vertices when M is nickel (*3*)].

VI. Partially Fused Polyhedra: Structures Related to the Tetracarbon Carboranes and Metallacarboranes

Carbon-rich carboranes, as defined for purposes of this chapter, are polyhedral borane cages containing three or more (usually four) carbon atoms. Ordinary bis(carboranyl) metal complexes of the type $(R_2C_2B_nH_m)_2M$ are excluded from this category because the individual MC_2B_n cage systems have only two carbons. However, there is an intermediate, borderline class of complexes in which the carborane ligands are linked by more than a common metal atom and which can be described as "partially fused." One might suspect that such species are related, somehow, to the oxidative fusion process described previously; such a relationship has already been found in at least one case.

A. $MFeC_4B_8$ "Wedged" Complexes (M = Co, Fe, Ge, Sn)

Reactions of the red iron complex $[(CH_3)_2C_2B_4H_4]_2FeH_2$ or its conjugate base anion with a variety of metal reagents result in the introduction of a second metal atom to give a wedged complex (*53, 58*).

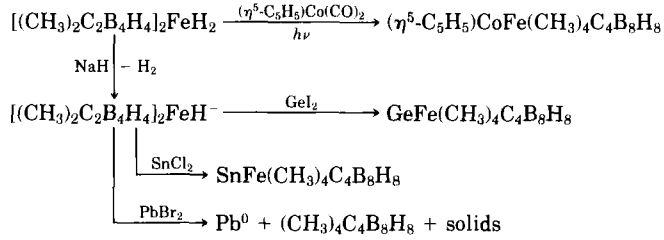

The cobalt–iron complex has been shown by X-ray crystallography (*55*) to have the structure depicted in Fig. 36a, wherein the cobalt displaces a BH unit into a wedging position. In the germanium–iron and tin–iron compounds, however, NMR evidence (*58*) suggests that the main-group metal occupies the wedging location (Fig. 36b). Such a structure has, in fact, been established for the diiron complex $[(CH_3)_2C_2B_4H_4]_2Fe_2 \cdot (OCH_3)_2C_2H_4$, which is described in Section IV,A (see Fig. 14). This latter compound, on exposure to O_2 or $FeCl_3$, undergoes rapid oxidative fusion to give $(CH_3)_4C_4B_8H_8$, but the three wedged, dimetallic species just listed are air stable and thus far have not shown any propensity to fuse.

In both of the established structures of wedged-type complexes (Figs. 14 and 36a), the bond distances from the wedging atom to the car-

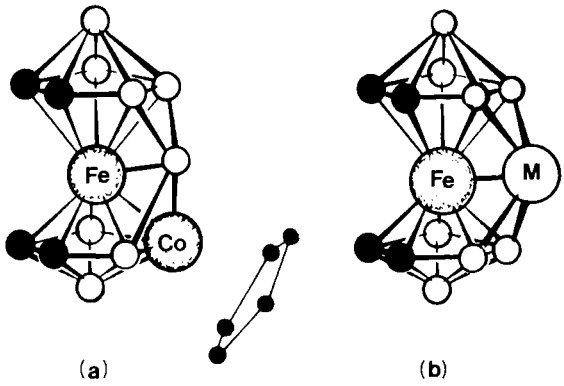

FIG. 36. (a) Established structure of $(\eta^5\text{-}C_5H_5)CoFe(CH_3)_4C_4B_8H_8$ (*55*). (b) Proposed structure of $MFe(CH_3)_4C_4B_8H_8$ (M = Ge, Sn) (*58*). Reprinted from *Inorg. Chem.* **16**, 3094. Copyright 1977 American Chemical Society. ○, BH; ●, CCH_3.

borane ligands are relatively long, although still well within bonding range. The chemistry of the wedged species has scarcely been examined as yet but should prove interesting; the wedging metal (or boron) atoms occupy comparatively exposed sites and are likely to be highly reactive toward attacking reagents. The almost instantaneous oxidation of $[R_2C_2B_4H_4]_2Fe_2L_2$ (L = THF or $\frac{1}{2}$DME) to form $R_4C_4B_8H_8$, noted earlier, is in line with this idea.

B. A Metallacarborane with a Fluxional Interligand B—B Linkage

The complex (*14*) to be described here is structurally unique in boron chemistry, although it is related to other known species. Treatment of a THF solution of $Na^+(CH_3)_2C_2B_4H_5^-$ with $CoCl_2$ and $Li^+C_5(CH_3)_5^-$ forms, as expected, the *closo*-cobaltacarboranes 1,2,3-$[C_5(CH_3)_5]$-$Co(CH_3)_2C_2B_4H_4$ and 1,7,2,3-$[C_5(CH_3)_5]_2Co_2(CH_3)_2C_2B_3H_3$ (the latter compound is a triple-decker sandwich), in analogy with the corresponding $C_5H_5^-$ reaction (*25*). However, with $C_5(CH_3)_5^-$ an additional product, *having no known $C_5H_5^-$ counterpart,* is also obtained in a yield of a few percent. An X-ray crystal-structure determination on this complex (*14*), $[\eta^5\text{-}C_5(CH_3)_5]_2Co_3(CH_3)_4C_4B_8H_7$, revealed that it consists of two CoC_2B_4 cages coordinated to a common cobalt atom, thereby forming two closo 8-vertex $Co_2C_2B_4$ polyhedra. The extraordinary feature, however, is that one boron atom on each cage lacks a terminal hydrogen, and these borons are directly linked to each other [bond distance 1.758(5) Å]. This structure is shown in Fig. 37.

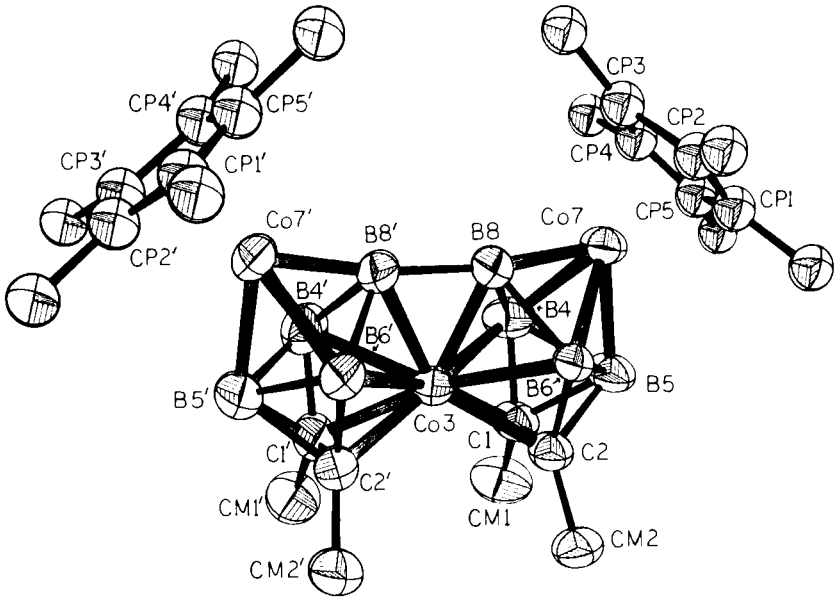

FIG. 37. Structure of $[\eta^5\text{-}C_5(CH_3)_5]_2Co_3(CH_3)_4C_4B_8H_7$ (*14*). Reprinted from *J. Am. Chem. Soc.* **103,** 1399. Copyright 1981 American Chemical Society.

The molecule possesses one nonterminal hydrogen atom that was not found in the X-ray study but that is presumed from indirect X-ray evidence to be located, in the solid state, in a pocket between the two cages, as suggested schematically in Fig. 38a. In $CDCl_3$ or C_6D_6 solution the interpolyhedral B—B bond is cleaved, thereby opening two sites available for terminal hydrogen bonding; the extra hydrogen atom apparently flips back and forth between these two boron atoms, as shown in Fig. 38b. A symmetrical B—H—B bridged arrangement (Fig. 38c) is evidently excluded both in the solid and solution states as a static structure, but it may well represent a transition state for the interchange shown in Fig. 38b. These conclusions are based on detailed ^{11}B- and ^1H-NMR studies, which have been described elsewhere (*14*).

Although this species is presently unique [there is no other example of a biscarboranyl *commo*-metallacarborane with a direct bond between the ligands], it may represent an early stage in the oxidative ligand-fusion process. This particular compound is air stable and has not exhibited any tendency to fuse, which is perhaps explained by the presence of the bulky $C_5(CH_3)_5$ ligands. Conceivably, however, somewhat similar interligand linkage may occur during the actual fusion of complexes such as $[R_2C_2B_4H_4]_2FeH_2$.

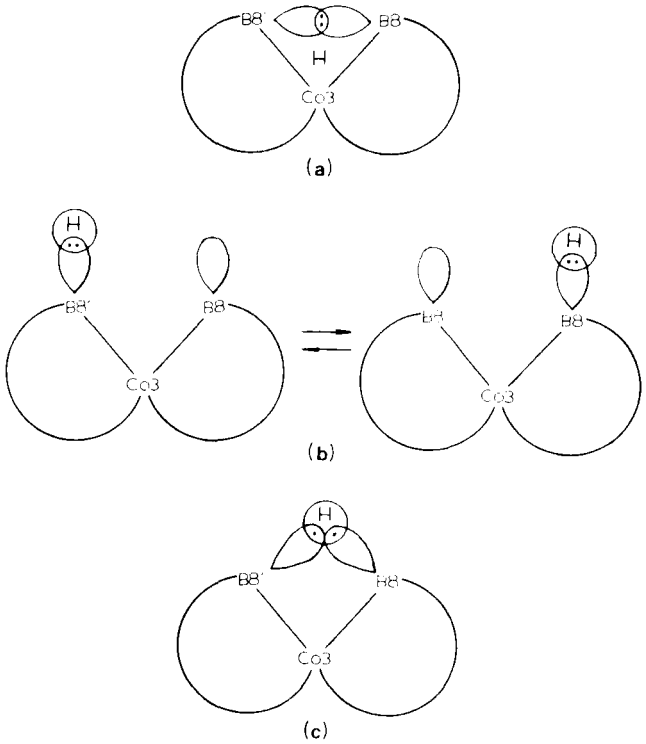

FIG. 38. Proposed sites for location of the fluxional hydrogen atom in the linked-cage tricobalt complex shown in Fig. 37. (a) Hydrogen in the vicinity of the central cobalt [Co(3)], with a direct B(8)—B(8′) link (solid-state structure). (b) Hydrogen exchanged between terminal positions on B(8) and B(8′) (proposed solution structure). (c) Three-center interligand B—H—B bridge. There is no evidence for structure (c), but it may exist as a transient during the tautomerism shown in (b) (*14*). Reprinted from *J. Am. Chem. Soc.* **103,** 1399. Copyright 1981 American Chemical Society.

VII. Structural Trends in Carbon-Rich Carborane Frameworks

Given the wide variety of geometric forms exhibited by the known four-carbon carborane and metallacarborane cage systems, there is every reason to believe many more novel structures will be encountered. This extraordinarily complex stereochemistry can be traced to several factors: (1) the importance of local bonding effects in systems with high heteroatom content; (2) the fact that most of these species were obtained under mild conditions that preclude rearrangement, allowing kinetic stabilization of unusual bonding patterns; and (3) the

presence of $2n + 4$ or $2n + 6$ skeletal electrons in most of the systems, leading (as predicted by Wade's rules) to open-cage geometries.

At this writing, over two dozen compounds in this class have been characterized by X-ray diffraction. These species, discussed in earlier sections, contain zero to two metal atoms per cage, and the metals represented are iron, cobalt, and nickel. Is anything to be gained by examining this somewhat random collection of molecules for structural trends? In a rigorous sense, probably not; on the other hand, clues to important principles of structure and bonding have often been first noted on a purely empirical plane, supported only later by careful theoretical analysis. This is particularly so in boron chemistry, where, for example, Stock's classifications of boranes into B_nH_{n+4} and B_nH_{n+6} groups (*83*) long preceded even the determination of molecular structures, let alone the development of bonding principles.

Two obvious patterns to be noted involve the carbon and metal locations, particularly with respect to the open faces. Figure 39 depicts in schematic fashion the open-face arrangements in the established four-carbon carborane and metallacarborane structures [the only closo framework, that of $(C_5H_5)_2Fe_2(CH_3)_4C_4B_8H_8$, isomer **VIII** (Fig. 34), lacks an open face and is omitted]. A conspicuous feature of these diagrams is the presence of three or four carbon atoms in most cases; indeed, 90% of the skeletal carbons in the structures under discussion occupy locations on an open rim. In the *nonmetal* species (Fig. 39a–d), *all* carbon atoms are on the rim.

In part, the tendency of carbon to occupy open-face vertices simply reflects a well-known rule that carbon prefers low-coordinate situations in borane clusters. Thus, although the skeletal coordination of carbon in the entire group of crystal structures ranges from two to five, nearly two-thirds of these carbons are four-coordinate with respect to the cage. In addition, one can expect the bonding around an open rim to be somewhat more localized than in the remainder of the cage. Both low coordination and localized electron distribution are favorable for carbon, a highly electronegative element that tends to adopt hydrocarbon-like bonding modes as far as possible (note, for example, the several structures in which a former framework carbon atom has been converted to an —RCH— bridging group via acquisition of hydrogen).

How does carbon manage to adopt low-coordinate rim locations so much of the time, given our assumption that extensive cage rearrangement is unlikely under the conditions of synthesis for most of these species? A likely explanation is that open faces are created merely by stretching particular edges of a polyhedral cage to nonbonding distances; this can be accomplished with relatively little atomic move-

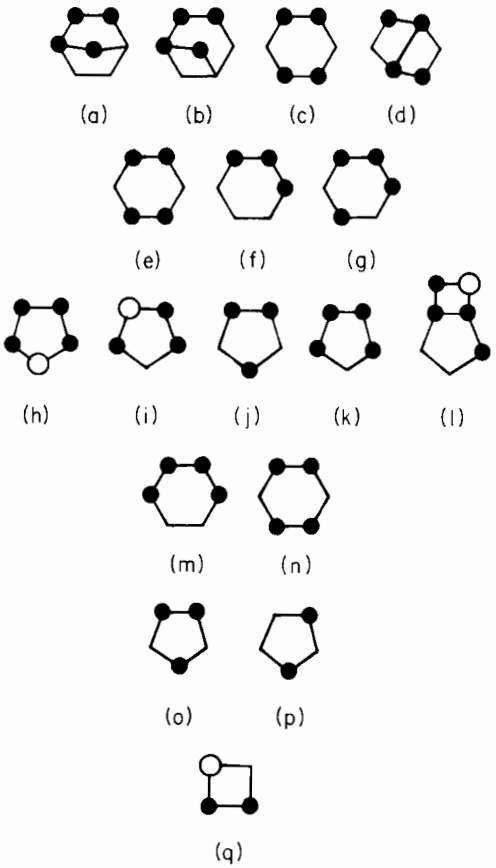

FIG. 39. Observed open-face geometries in structurally established C_4 carboranes and metallacarboranes. Systems: (a)–(d), nonmetal; (e)–(l), one-metal; (m)–(q), two-metal. Each diagram depicts the pattern of occupancy of vertices on the open face(s) by carbon, boron, and metal atoms. ●, Carbon; ∠, boron; ○, metal. Deviations from planarity of the open faces are ignored, as are bridging hydrogens and all atoms not located on open faces. (a) $(CH_3)_4C_4B_7H_8Br$ (Fig. 20). (b) $(CH_3)_4C_4B_8H_9^-$ (Fig. 17). (c) $(C_2H_5)_4C_4B_8H_8$ (*87*). (d) $(CH_3)_4C_4B_8H_8$ (Fig. 12) and $(C_5H_5)Fe(C_5H_4)$—$(CH_3)_4C_4B_8H_7$ (Fig. 13). (e) $(C_5H_5)Co(CH_3)_4C_4B_7H_7$, isomer **I** (Fig. 26) and $(C_5H_5)Co(C_6H_5)_4C_4B_3H_3$ (Fig. 9). (f) $(C_5H_5)Fe(CH_3)_4C_4B_7H_8$ (Fig. 30, **5**). (g) $(C_5H_5)Co(CH_3)_4C_4B_7H_7$, isomer **III** (Fig. 35) and $(C_5H_5)Cr(C_2H_5)_4C_4B_7H_7$ (Fig. 32). (h) $(C_5H_5)Co(CH_3)_4C_4B_6H_6$, isomer **II** (Fig. 27). (i) $[(C_6H_5)_2PCH_2]_2Ni(CH_3)_4C_4B_8H_8$ (Fig. 29). (j) $(C_5H_5)Cr(C_2H_5)_4C_4B_8H_8$ (Fig. 32). (k) $(C_5H_5)Co(CH_3)_4C_4B_6H_6$, isomer **I** (Fig. 27). (l) $(C_5H_5)Co(CH_3)_4C_4B_7H_7$, isomer **II** (Figs. 28 and 35). (m) $(C_5H_5)_2Co_2C_4B_6H_{10}$, isomer **VII** (Fig. 24). (n) $(C_5H_5)_2Co_2(CH_3)_4C_4B_6H_6$, isomer **V** (Fig. 23). (o) $(C_5H_5)_2Fe_2(CH_3)_4C_4B_8H_8$, isomer **I** (Fig. 31). (p) $(C_5H_5)_2Fe_2$-$(CH_3)_4C_4B_8H_8$, isomer **V** (Fig. 33). (q) $(C_5H_5)_2Fe_2(CH_3)_4C_4B_8H_8$, isomer **II** (Fig. 31).

ment and is clearly, in general, a low-energy process [the fluxional $R_4C_4B_8H_8$ carboranes (Section IV,B) provide an excellent illustration of this point]. Hence, in most C_4 carborane and metallacarborane cage systems, the skeletal carbons can be placed in low-coordinate and/or open-rim locations without actual migration of atoms on the polyhedral surface. Indeed, in the 14-vertex $(C_5H_5)_2Fe_2(CH_3)_4C_4B_8H_8$ complexes **I**, **II**, and **V** (Fig. 33) this is achieved by appropriate edge-stretching *despite* the fact that the $2n + 2$ framework electrons favor closo polyhedral geometry.

The placement of metal atoms requires little discussion. With one exception, all metals in this particular group of clusters are five- or six-coordinate; only in $(C_5H_5)Co(CH_3)_4C_4B_6H_6$, isomer **II** (Fig. 27), is the metal atom adjacent to as few as four skeletal atoms. This observation is consistent with a general pattern in metallacarborane structures (*22*), particularly those in which iron and cobalt are involved. Metal atoms tend to locate adjacent to carbon; each metal in these structures has at least two neighboring carbon atoms in the framework. In part, this merely reflects the high molar density of carbon in these C_4 clusters; in addition, however, metal insertion into open carborane cages almost inevitably takes place at the open face, and, as we have noted, such faces are usually rich in carbon.

VIII. Concluding Observations

The hypothetical experiment mentioned in Section I, in which boron atoms in a polyhedral $C_2B_{10}H_{12}$ carborane are successively replaced by carbon until one has $C_{12}H_{12}$, is of course well beyond the current state of the art in synthetic boron chemistry; for that matter, even theoretical predictions of the various intermediate structures are not presently feasible on any rigorous basis. What *has* happened, however, is that a particular stage in this series, $C_4B_8H_{12}$, has been fortuitously obtained in the form of tetraalkyl derivatives and studied extensively. Thus we have, basically, a picture of the consequences of replacing *some* of the boron in a 12-vertex polyhedron with carbon, and it is a complex picture indeed, particularly when the metallacarborane complexes are included.

As the carbon content of the cage is further increased, it would be reasonable to expect the main structural trends observed in the four-carbon systems to be extended; thus in a $R_6C_6B_6H_6$ polyhedron at least some of the framework carbon atoms should adopt hydrocarbon-like, localized, four-coordinate bonding modes. A particularly interesting

question is whether such cages would exhibit isomerism and fluxional behavior akin to that of the C_4B_8 systems described in this chapter. No carboranes having more than four skeletal carbon atoms have been characterized [although evidence for six- and eight-carbon species has been reported (*12*)], and for the foreseeable future it will be up to the synthetic chemist to resolve such questions.

ACKNOWLEDGMENTS

It is a pleasure to note the generous support of the Office of Naval Research and the National Science Foundation for the work at the University of Virginia described in this chapter, as well as the efforts of the many co-workers who are named in the references. I am grateful to T. Leon Venable for reading the manuscript and offering many helpful suggestions.

REFERENCES

1. Berger, H. O., Noeth, H., and Wrackmeyer, B., *Chem. Ber.* **112,** 2884 (1979).
2. Binger, P., *Tetrahedron Lett.* p. 2675 (1966).
3. Bowser, J. R., Bonny A., Pipal, J. R., and Gimes, R. N., *J. Am. Chem. Soc.* **101,** 6229 (1979).
4. Brown, L. D., and Lipscomb, W. N., *Inorg. Chem.* **16,** 2989 (1977).
5. Camp, R. N., Marynick, D. S., Graham, G. D., and Lipscomb, W. N., *J. Am. Chem. Soc.* **100,** 6781 (1978).
6. Chamberland, B. L., and Muetterties, E. L., *Inorg. Chem.* **3,** 1450 (1964).
7. Churchill, M. R., and DeBoer, B. G., *Inorg. Chem.* **12,** 2674 (1973).
8. Dixon, D. A., Kleier, D. A., Halgren, T. A., Hall, J. H., and Lipscomb, W. N., *J. Am. Chem. Soc.* **99,** 6226 (1977).
9. Dustin, D. F., Evans, W. J., Jones, C. R., Wiersema, R. J., Gong, H., Chan, S., and Hawthorne, M. F., *J. Am. Chem. Soc.* **96,** 3085 (1974).
10. Evans, W. J., and Hawthorne, M. F., *J. Chem. Soc., Chem. Commun.* p. 38 (1974).
11. Evans, W. J., Jones, C. J., Stibr, B., and Hawthorne, M. F., *J. Organomet. Chem.* **60,** C27 (1973).
12. Fehlner, T. P., *J. Am. Chem. Soc.* **102,** 3424 (1980).
13. Finster, D. C., and Grimes, R. N., *J. Am. Chem. Soc.* **103,** 2675 (1981).
14. Finster, D. C., Sinn, E., and Grimes, R. N., *J. Am. Chem. Soc.* **103,** 1399 (1981).
15. Franz, D. A., and Grimes, R. N., *J. Am. Chem. Soc.* **93,** 387 (1971).
16. Freyberg, D. P., Weiss, R., Sinn, E., and Grimes, R. N., *Inorg. Chem.* **16,** 1847 (1977).
17. Greenwood, N. N., and Thomas, B. S., "The Chemistry of Boron." Permagon, Oxford, 1973.
18. Grimes, R. N., *Acc. Chem. Res.* **11,** 420 (1978).
19. Grimes, R. N., *Acc. Chem. Res.* **16,** 22 (1983).
20. Grimes, R. N., *Ann. N.Y. Acad. Sci.* **239,** 180 (1974).
21. Grimes, R. N., "Carboranes." Academic Press, New York, 1970.
22. Grimes, R. N., *in* "Comprehensive Organometallic Chemistry" (G. Wilkinson, F. G. A. Stone, and E. Abel, eds.), Vol. 1, Chapter 5.5. Pergamon, Oxford, 1982.

23. Grimes, R. N., *Coord. Chem. Rev.* **28,** 47 (1979).
24. Grimes, R. N., ed., "Metal Interactions with Boron Clusters." Plenum, New York, 1982.
25. Grimes, R. N., Beer, D. C., Sneddon, L. G., Miller, V. R., and Weiss, R., *Inorg. Chem.* **13,** 1138 (1974).
26. Grimes, R. N., and Bramlett, C. L., *J. Am. Chem. Soc.* **89,** 2557 (1967).
27. Grimes, R. N., Maxwell, W. M., Maynard, R. B., and Sinn, E., *Inorg. Chem.* **19,** 2981 (1980).
28. Grimes, R. N., Maynard, R. B., Sinn, E., and Long, G. J., *Abstr. Pap., 182nd Natl. Meet., Am. Chem. Soc.* Abstract INOR-10 (1981); see also Maynard, R. B., and Grimes, R. N., *J. Am. Chem. Soc.* **104,** 5983 (1982).
29. Grimes, R. N., Maynard, R. B., Sinn, E., Brewer, G., and Long, G. J., *J. Am. Chem. Soc.* **104,** 5987 (1982).
30. Grimes, R. N., Pipal, J. R., and Sinn, E., *J. Am. Chem. Soc.* **101,** 4172 (1979).
31. Grimes, R. N., Sinn, E., and Pipal, J. R., *Inorg. Chem.* **19,** 2087 (1980).
32. Hawthorne, M. F., Pilling, R. L., and Stokely, P. F., *J. Am. Chem. Soc.* **87,** 1893 (1965).
33. Herberich, G. E., Hengesbach, J., Kolle, U., Huttner, G., and Frank, A., *Angew. Chem., Int. Ed. Engl.* **15,** 433 (1976).
34. Herberich, G. E., Hengesbach, J., Kolle, U., and Oschmann, W., *Angew. Chem., Int. Ed. Engl.* **16,** 42 (1977).
35. Herberich, G. E., Hessner, B., Beswetherick, S., Howard, J. A. K., and Woodward, P., *J. Organomet. Chem.* **192,** 421 (1980).
36. Herberich, G. E., Hessner, B., Huttner, G., and Zsolnai, L., *Angew. Chem.* **93,** 471 (1981).
37. Hosmane, N. S., and Grimes, R. N., *Inorg. Chem.* **18,** 2886 (1979).
38. Hosmane, N. S., and Grimes, R. N., *Inorg. Chem.* **18,** 3294 (1979).
39. Hosmane, N. S., and Grimes, R. N., *Inorg. Chem.* **19,** 3482 (1980).
40. Howard, J. W., and Grimes, R. N. *Inorg. Chem.* **11,** 263 (1972).
41. Janousek, Z., Hermanek, S., Plesek, J., and Stibr, B., *Collect. Czech. Chem. Commun.* **39,** 2363 (1974).
42. Kaczmarczyk, A., Dobrott, R. D., and Lipscomb, W. N., *Proc. Natl. Acad. Sci. U. S. A.* **48,** 729 (1962).
43. Kaloustian, M. K., Wiersema, R. J., and Hawthorne, M. F., *J. Am. Chem. Soc.* **94,** 6679 (1972).
44. King, R. B., and Rouvray, D. H., *J. Am. Chem. Soc.* **99,** 24 (1977).
45. Lipscomb, W. N., "Boron Hydrides." Benjamin, New York, 1963.
46. Lipscomb, W. N., *Inorg. Chem.* **18,** 2328 (1979).
47. Lipscomb, W. N., *Science* **153,** 373 (1966).
48. Maddres, P. S., Modinos, A., Timms, P. L., and Woodward, P., *J. Chem. Soc., Dalton Trans.* p. 1272 (1975).
49. Marynick, D. S., and Lipscomb, W. N., *J. Am. Chem. Soc.* **94,** 8699 (1972).
50. Maxwell, W. M., Bryan, R. F., and Grimes, R. N., *J. Am. Chem. Soc.* **99,** 4008 (1977).
51. Maxwell, W. M., and Grimes, R. N., *Inorg. Chem.* **18,** 2174 (1979).
52. Maxwell, W. M., Miller, V. R., and Grimes, R. N., *Inorg. Chem.* **15,** 1343 (1976).
53. Maxwell, W. M., Miller, V. R., and Grimes, R. N., *J. Am. Chem. Soc.* **96,** 7116 (1974).
54. Maxwell, W. M., Miller, V. R., and Grimes, R. N., *J. Am. Chem. Soc.* **98,** 4818 (1976).
55. Maxwell, W. M., Sinn, E., and Grimes, R. N., *J. Am. Chem. Soc.* **98,** 3490 (1976).
56. Maxwell, W. M., Sinn, E., and Grimes, R. N., *J. Chem. Soc., Chem. Commun.* p. 390 (1976).

57. Maxwell, W. M., Weiss, R., Sinn, E., and Grimes, R. N., *J. Am. Chem. Soc.* **99,** 4016 (1977).
58. Maxwell, W. M., Wong, K.-S., and Grimes, R. N., *Inorg. Chem.* **16,** 3094 (1977).
59. Maynard, R. B., Sinn, E., and Grimes, R. N., *Inorg. Chem.* **20,** 1201 (1981).
60. Maynard, R. B., Sinn, E., and Grimes, R. N., *Inorg. Chem.* **20,** 3858 (1981).
61. Maynard, R. B., Wang, Z., Sinn, E., and Grimes, R. N., *Inorg. Chem.* **22,** in press (1983).
62. Middaugh, R. L., and Farha, F., Jr., *J. Am. Chem. Soc.* **88,** 4147 (1966).
63. Miller, V. R., and Grimes, R. N., *Inorg. Chem.* **11,** 862 (1972).
64. Miller, V. R., and Grimes, R. N., *J. Am. Chem. Soc.* **97,** 4213 (1975).
65. Mingos, D. M. P., *Nature (London), Phys. Sci.* **236,** 99 (1972).
66. Muetterties, E. L., ed., "Boron Hydride Chemistry." Academic Press, New York, 1975.
67. Onak, T. P., "Organoborane Chemistry." Academic Press, New York, 1975.
68. Onak, T. P., Drake, R. P., and Dunks, G. B., *Inorg. Chem.* **3,** 1686 (1964).
69. Onak, T. P., and Dunks, G. B., *Inorg. Chem.* **5,** 439 (1966).
70. Onak, T. P., and Wong, G. T. F., *J. Am. Chem. Soc.* **92,** 5226 (1970).
71. O'Neill, M. E., and Wade, K., *in* "Metal Interactions with Boron Clusters" (R. N. Grimes, ed.) Chapter 1. Plenum, New York, 1982.
72. Pasinski, J. P., and Beaudet, R. A., *J. Chem. Phys.* **61,** 683 (1974).
73. Pipal, J. R., and Grimes, R. N., *Inorg. Chem.* **17,** 6 (1978).
74. Pipal, J. R., and Grimes, R. N., *Inorg. Chem.* **18,** 257 (1979).
75. Pipal, J. R., and Grimes, R. N., *Inorg. Chem.* **18,** 263 (1979).
76. Pipal, J. R., and Grimes, R. N., *Inorg. Chem.* **18,** 1936 (1979).
77. Pipal, J. R., and Grimes, R. N., *J. Am. Chem. Soc.* **100,** 3083 (1978).
78. Plesek, J., and Hermanek, S., *Chem. Ind. (London)* p. 890 (1972).
79. Rudolph, R. W. *Acc. Chem. Res.* **9,** 446 (1976).
80. Siebert, W., *Adv. Organomet. Chem.* **18,** 301 (1980).
81. Siebert, W., and Bochmann, M., *Angew. Chem., Int. Ed. Engl.* **16,** 468 (1977).
82. Siebert, W., and El-Essawi, M. E., *Chem. Ber.* **112,** 1480 (1979).
83. Stock, A., "Hydrides of Boron and Silicon." Cornell Univ. Press, Ithaca, New York, 1933.
84. Thompson, M. L., and Grimes, R. N., *J. Am. Chem. Soc.* **93,** 6677 (1971).
85. Timms, P. L., *Acc. Chem. Res.* **6,** 118 (1973).
86. Tolpin, E. I., and Lipscomb, W. N., *Inorg. Chem.* **12,** 2257 (1973).
87. Venable, T. L., Maynard, R. B., Sinn, E., and Grimes, R. N., to be submitted for publication.
88. Wade, K., *Adv. Inorg. Chem. Radiochem.* **18,** 1 (1976).
89. Welch, A. J., private communication.
90. Williams, R. E., *Adv. Inorg. Chem. Radiochem.* **18,** 67 (1976).
91. Wong, K.-S., Bowser, J. R., Pipal, J. R., and Grimes, R. N., *J. Am. Chem. Soc.* **100,** 5045 (1978).
92. Zimmerman, G. J., Hall, L. W., and Sneddon, L. G., *Inorg. Chem.* **19,** 3642 (1980).
93. Zimmerman, G. J., and Sneddon, L. G., *Inorg. Chem.* **19,** 3650 (1980).